Royal Netherlands
Meteorological Institute
*Ministry of Infrastructure and the
Environment*
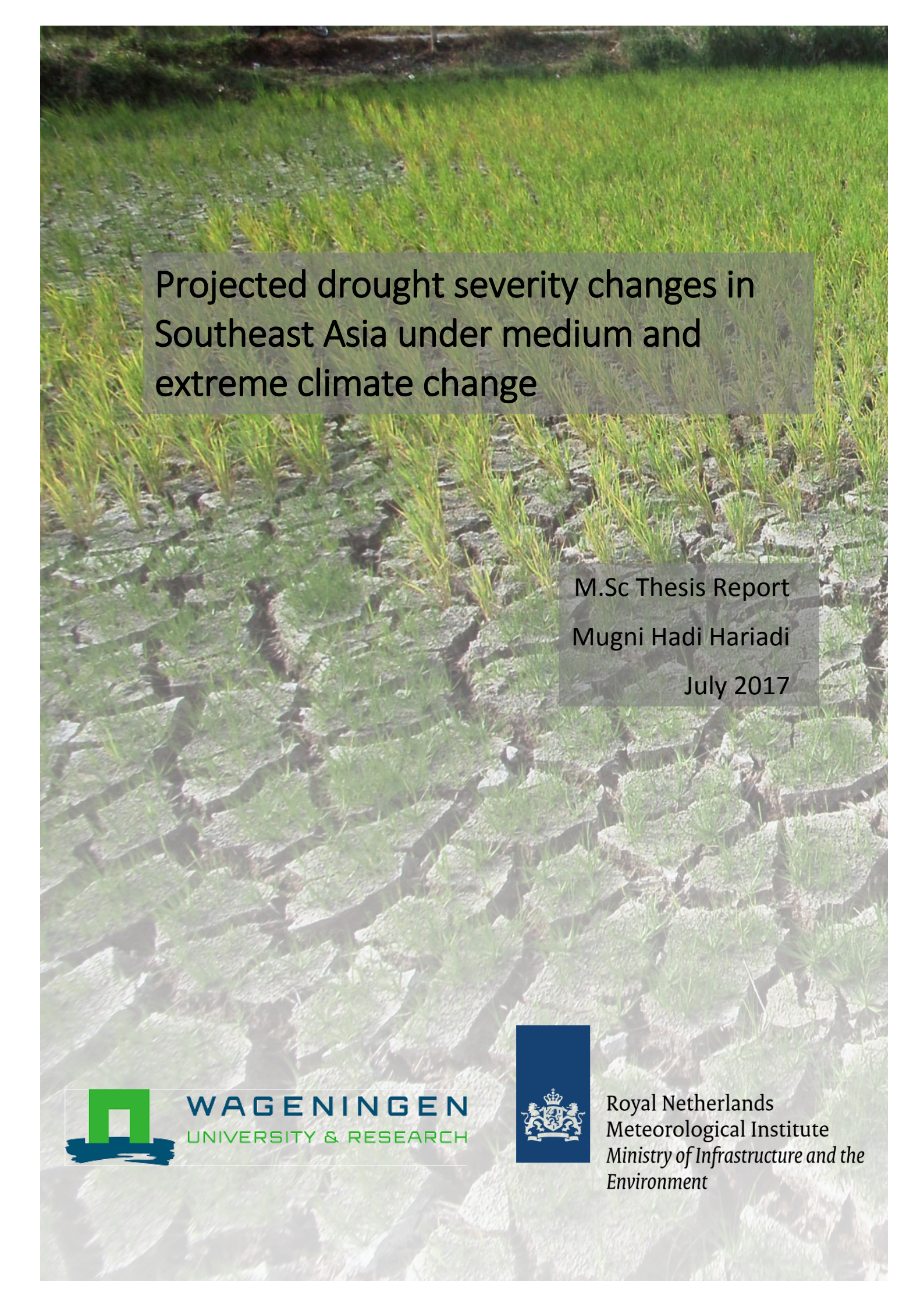
Projected drought severity changes in Southeast Asia under medium and extreme climate change

Mugni Hadi Hariadi

Projected drought severity changes in Southeast Asia under medium and extreme climate change

M.Sc Thesis Report

Mugni Hadi Hariadi

July 2017

WAGENINGEN
UNIVERSITY & RESEARCH

Royal Netherlands
Meteorological Institute
*Ministry of Infrastructure and the
Environment*

Projected drought severity changes in Southeast Asia under medium and extreme climate change

Mugni Hadi Hariadi

July 2017

M.Sc Thesis

Master Program Climate Studies

Meteorology and Air Quality Group

Wageningen University

Supervisors:

Prof. Albert Klein Tank (WUR and KNMI)

Gerard van der Schrier (KNMI)

WAGENINGEN
UNIVERSITY & RESEARCH

Royal Netherlands
Meteorological Institute
*Ministry of Infrastructure and the
Environment*

Abstract

The El Nino-Southern Oscillation (ENSO) is the main driver of seasonal conditions in the Southeast Asia region and the El-Nino (EN) is related to the dry period that affects the food security in the region. The EN of 1997 was recorded as the strongest ever El-Nino and brought the driest period for the region on record, with the EN of 1982 a close second. In this thesis, we analyse the impact of reduced rainfall and the extreme high temperatures associated with EN events on drought conditions, by comparing the drought conditions of EN 1982 and EN 1997 as strong EN events, with EN 2015 as a moderate EN that had extreme warm temperatures by calculating the self-calibration Palmer drought severity index (scPDSI). With the trend of increasing temperatures in the future and the associated increased atmospheric water demand (the "thirst of the atmosphere"), the same drought severity level, such as EN 1997, can occur even with lower precipitation anomaly. To look into this issue, Coordinated Regional Climate Downscaling Experiment (CORDEX) Southeast Asia (CORDEX-SEA) simulation are analysed. CORDEX-SEA is regional climate model (RCM) dataset for Southeast Asia region. In this case we used CORDEX-SEA which used the Hadley Centre Global Environmental Model version 2–Atmosphere–Ocean (HadGEM2–AO) as boundary conditions for the regional model. The empirical quantile mapping (eQM) method was selected to bias corrected CORDEX-SEA dataset using gridded observation dataset (SA-OBS), we found that the method performed better compared to scaling and gamma quantile mapping (gQM) methods. Assuming EN 1997 as the driest period and representing it as a 30-year return period event in the model data, we show that such droughts will be common in the far future (2070-2100) period under extreme climate change. Furthermore, the results show that not only drought will be more severe in the future, but also that more areas will be affected by drought. The driest year in the future is documented in this thesis, and it is likely that under extreme climate change in far future period that in the driest year almost half of the region will be affected by extreme drought. In general, areas around the equator, like most of Indonesian regions, will have a higher drought severity change in the future compared to other areas. The report will end with a brief discussion on the validity of the assumptions and approach, and suggestions for future work.

Contents

List of Figures

1. INTRODUCTION

Dry periods are frequent occurrence in Southeast Asia, especially in Indonesia, in concurrence with the El Nino (EN) phenomenon. However, it does not always cause severe droughts. Nonetheless, drought affects many sectors of life, especially agriculture, which can lead to a food insecurity crisis (Syaukat, 2011). The late onset of the rainy season, for example, triggers a high risk that the coming second-season harvest will fail (Van Der Schrier et al., 2016). Drought will reduce the availability of water and household access to clean drinking water and sanitation. This is also a main concern affecting large populations.

The strongest EN phenomenon experienced in recent history was recorded between March 1997 until February 1998. During this period, almost every region of Indonesia measured rainfall under the 10th percentile, and most of the rainfall stations over the country recorded their lowest rainfall ever (Kirono et al. ,1999). Regarding the seasonal variation of the precipitation in Indonesia, Kirono et al. (1999) stated that the largest impact of the EN year was during the dry season, which is from June to November 1997, followed by a reduced impact during the wet season, which is from December 1997 to February 1998. FAO and the Indonesian Biro of Statistic (BPS) recorded that due to EN 1997, rice production in the year of 1998 decreased by 3.6% from the previous year, and was 6% below the production of 1996. Furthermore, it is 11% below the official target for 1998.

There are two types of EN's that have been suggested, based on whether the maximum sea surface temperature (SST) anomalies are located in the Eastern Pacific (EP) or the central of Pacific (CP) (Jiménez-Muñoz et al., 2016). Firstly, the EN that is characterized with a maximum anomaly in the EP is called canonical EN, strong EN's such as in 1982 and 1997 had this characteristic. Secondly, the EN that is characterized with a maximum anomaly in the CP generates weaker EN events, such as the last EN in 2015, which is usually known as *Modoki EN* (Jiménez-Muñoz et al., 2016). For the Indonesian region, every EN event caused a precipitation anomaly in most areas, comparing the 1997 to 2015, the anomaly of the rainfall that was caused by EN 2015 is less compared to EN 1997 (Ministry of Agriculture, 2016). Indonesia food security monitoring bulletin 2015 showed that rainfall is 70-50% less with respect to normal for some areas in the south part of Sumatera and west Java in 1997 EN, but in EN 2015 those areas had less anomaly with around 30-50% less from its normal.

However, 2015 not only recorded an EN but it was also globally recorded as the warmest year in the past 35 years (Nasa, 2015). Global temperature in 2015 was 0.13^OC higher than in 2014 as the previous record. It was only in 1998, that global temperature record is higher than the previous record by this much before (Nasa, 2015).

The rainfall anomaly in the 2015 EN is less compared to the 1997 EN, but the soil water availability anomaly can be different. The increase of temperature by 1^OC will increase the water holding capacity of air by about 7%, which will increase the potential evapotranspiration (Trenberth, 2011). As a result, the high temperature will affect the soil water availability. Jiménez-Muñoz et al. (2016) analysed this issue by calculating the self-calibration Palmer Drought Severity Index (scPDSI) for the Amazon region. They found that the pattern of the area that was affected by drought for 2015 is different to that of 1997 and 1982. In 2015, the areas that were affected by drought are more concentrated in the eastern part of the region. Although their areas are less widespread compared to 1997 and 1982, the areas that saw dry condition in 2015 was more severe than the other EN years.

Drought and its projection in the future are chosen as the main topics in this study. The scPDSI index was calculated on historical and future periods to describe the drought condition in different EN years and different periods. The scPDSI was chosen in this thesis to describe the drought condition because beside precipitation scPDSI index include evapotranspiration (estimated from temperature) in the calculation. Moreover, it has strong relationship with river streamflow and soil moisture (Dai, 2011).

The research questions for this thesis are:
1. What is the best bias correction method to bias corrected Regional Climate Model (RCM) for Southeast Asia region?
2. How is the condition of drought during EN 2015 compared to EN 1997 and EN 1982?
3. How is the drought projected for the future?
    a. How will severity and spatial extent of drought in Southeast Asia change in the future compared to the historical period?
    b. How frequent will drought conditions, such as EN 1997 and EN 1982, occur in the future?
    c. How will severity and spatial extent of the drought of 30 years and 15 years return periods in Southeast Asia change in the future compared to a historical period?

In this research, the future conditions are represented by Representative Concentration Pathways (RCP) 4.5 and 8.5. The RCP4.5 (intermediate emissions) represents a medium climate change where radiative forcing is stabilized at approximately 4.5 W/m2 after 2100. Meanwhile, RCP8.5 represents an extreme climate change, where radiative forcing reaches >8.5 W/m2 by 2100 and continues to rise for some amount of time (Van Vuuren, 2011). Due to limited regional climate model (RCM) data available for Southeast Asia, one dataset was used for future climate projection. Therefore, this research did not include the range of uncertainty from the different climate models. In this thesis, the 30-years and 15-years return periods of drought are used to represent the condition of EN 1997 and EN 1982 in RCM data. This is by assuming that drought in the strongest EN (1997) was the most severe drought in 30 years of historical period and drought in EN 1982 was the second most severe drought.

In addition, one of three bias correction methods was selected for bias corrected RCM data. Turco et. al (2015) found that empirical quartile mapping (eQM) and gamma quantile mapping (gQM) methods perform better compared to scaling method, for bias correcting RCM data over the Greater Alpine Region. These three methods are also further compared in this study and the most optimal method is selected.

In the future, a smaller anomaly of rainfall and projected higher evaporation can potentially lead to a higher severity of drought. The IPCC report of Working Group (WG) II stated with confidence, that in Asia the increased risk of drought relating to water and food shortage will lead to malnutrition over the region (IPCC, 2014). It would be very useful to have more information about drought severity and the frequency in the future under different IPCC RCP scenarios for this region. This information is needed for adaptation strategies, especially in the food security sector.

2. METHODOLOGY

2.1   Methods

The research is divided into 2 main phases, namely, data preparation and drought analysis (Figure 1). The data preparation phase is primarily about selecting the best bias correction methods. In this phase, 10 grid cells (for precipitation) and 6 grid cells (for temperature) from Southeast Asia gridded observation dataset (SA-OBS) are selected for the analysis. The selected grid cells have observation station(s).

Three methods of bias correction that are applied in this analysis are scaling method, empirical quantile mapping method (eQM) and gamma quantile mapping method (gQM) (Table 1). Scaling and eQM methods are applied for precipitation and temperature data, and gQM method is applied for precipitation only (Table 1).

Table 1. Bias correction methods

Methods	Application	Information
Scaling	Precipitation and Temperature	The correction consists of the scaling the simulation with the difference between the mean of the observations and the simulation in the training period (Teutcshbein and Seibert, 2012; Fang et al., 2015)
eQM	Precipitation and Temperature	In the eQM technique, the transfer function is constructed from CDFs (cumulative distribution functions) of the model and the observation (Gudmundsson et al., 2012; and Wilcke et al., 2013).
gQM	Precipitation only	The gQM method is based on the initial assumption that both observed and simulated intensity distributions are well approximated by the gamma distribution (Piani et al., 2010).

Bias correction of RCM data using SA-OBS is done for the period of 1981-2005. Cross validation (leave out one year) technique is applied in the bias correction using *downscaleR* R package, developed by Santander Group (https://github.com/santanderMetGroup/downscaleR). Furthermore, performances of the methods were presented by verification diagrams such as empirical cumulative distribution function (ECDF) plot and quantile-quantile plot (QQplot).

CDF is a non-parametric estimator. ECDF plot is a graph that we can use to evaluate the fit of a distribution to our data, estimate percentiles, and compare different sample distributions. An empirical CDF plot shows the following: Plots each unique value vs the percentage of values in the sample that are less than or equal to it, and connects the points with a stepped line (Wilks, 2011). QQplot is a visual way to compare two marginal cumulative probability distributions by plotting model quantiles against observation quantiles (Wilks, 2011).

The second phase is the drought analysis. There are two scPDSI calculations in this phase using *pdsi* R package, developed by Cszang (https://github.com/cszang/pdsi). The first scPDSI calculation is from SAOBS precipitation (Van Den Besselaar et al., 2016) combined with CRU TS4 temperature (Harris et al., 2014). This calculation was used to answer the second research question: "How is the condition of drought during EN 2015 compared to EN 1997 and EN 1982?". The second scPDSI calculation,

RCM data was bias corrected using bias correction method that was selected in the first phase. Later, the bias corrected data was used to calculate scPDSI from the model. This calculation was used to answer the third research question related with drought projection in the future.

Drought condition (level severity and areas) in different EN events is analysed. Furthermore, return period of drought conditions in EN events is calculated based on percentage area affected by moderate-extreme drought. Hereafter, the frequency of year in the future that extended the driest year in historical were calculated to analyse the return period change. In addition, the driest year for every period was displayed to analyse the severity change on extreme year in the future.

The flow work of the research is presented in the figure below.
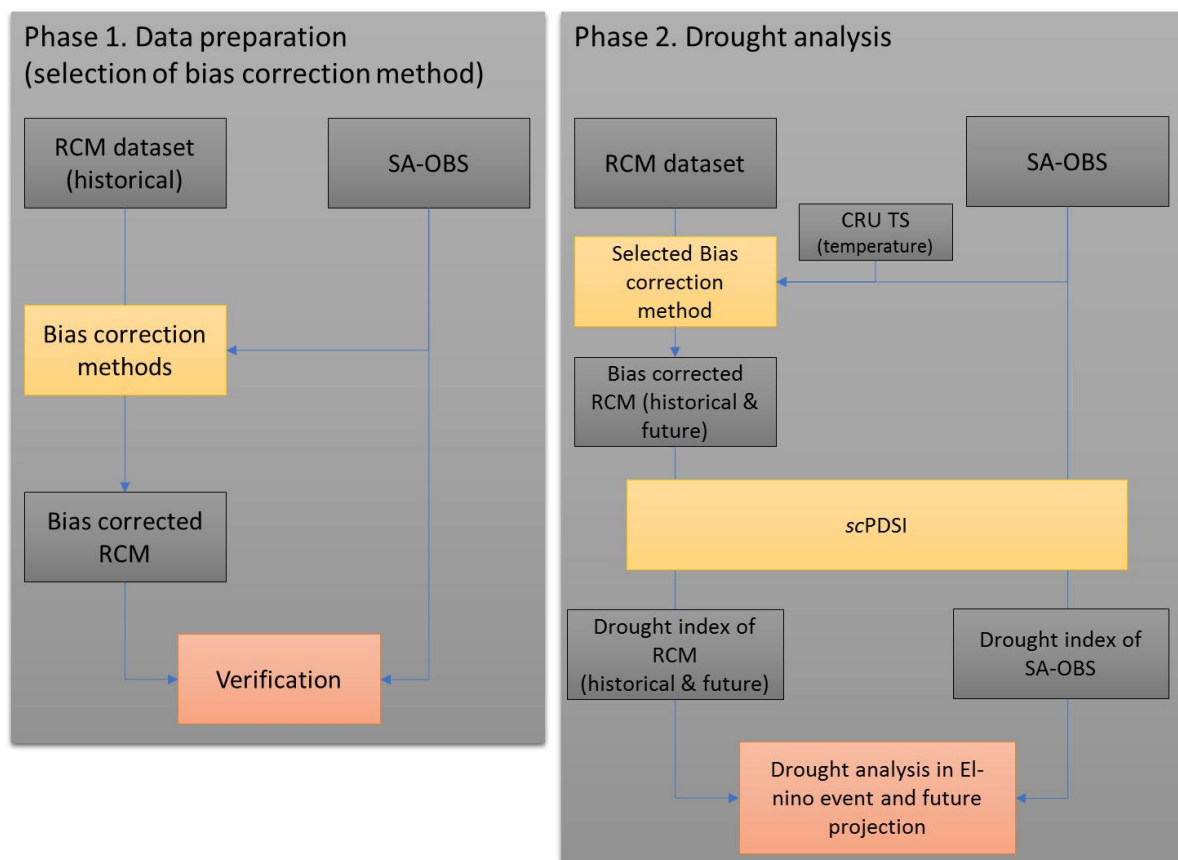
Figure 1. Flow work of the research

2.2 Data

2.2.1 CORDEX-SEA 25 km (RCM for Southeast Asia region)

In October 2013, the Asia-Pacific Network (APN) collaborating with seven countries (i.e., Indonesia, Malaysia, the Philippines, Thailand, Vietnam, Cambodia and Lao PDR) developed The Southeast Asia Regional Climate Downscaling (SEACLID). Furthermore, SEACLID initiated the Coordinated Regional Climate Downscaling Experiment (CORDEX) Southeast Asia (CORDEX-SEA), a high-resolution dynamic downscaling for the Southeast Asia domain (Figure 2). The aim of CORDEX-SEA is to provide an improved high-resolution climate project information for the local hydrological and agriculture sectors (Yang, 2015). Besides the institutions mentioned earlier, there is an external institution from outside the Southeast Asia region that also joined CORDEX-SEA, which is The Asia-Pacific Economic Cooperation Climate Centre (APCC). APCC has provided high-resolution climate projection on

resolution 0.25◦ by 0.25◦. The RCM dataset is available for historical periods (1971-2005), near future periods (2021-2050) and far future periods (2071-2100). The future period data is available under RCP4.5 and RCP8.5. APCC's CORDEX-SEA is performed using the regional Weather Research and Forecasting (WRF3.5) model which was developed by Skamarock et al. (2008). WRF3.5 is powered by the European Centre for Medium-Range Weather Forecasts (ECMWF) reanalysis (ERA)-Interim dataset, as well as the current climate and future projections of the Hadley Centre Global Environmental Model version 2–Atmosphere–Ocean (HadGEM2–AO) (Yang, 2015)).

This research uses precipitation and temperature of RCM from APCC's CORDEX-SEA on a 0.25◦ resolution. The data is available at http://cis.apcc21.org/opendap/CORDEX-SEA/SEA-25/.
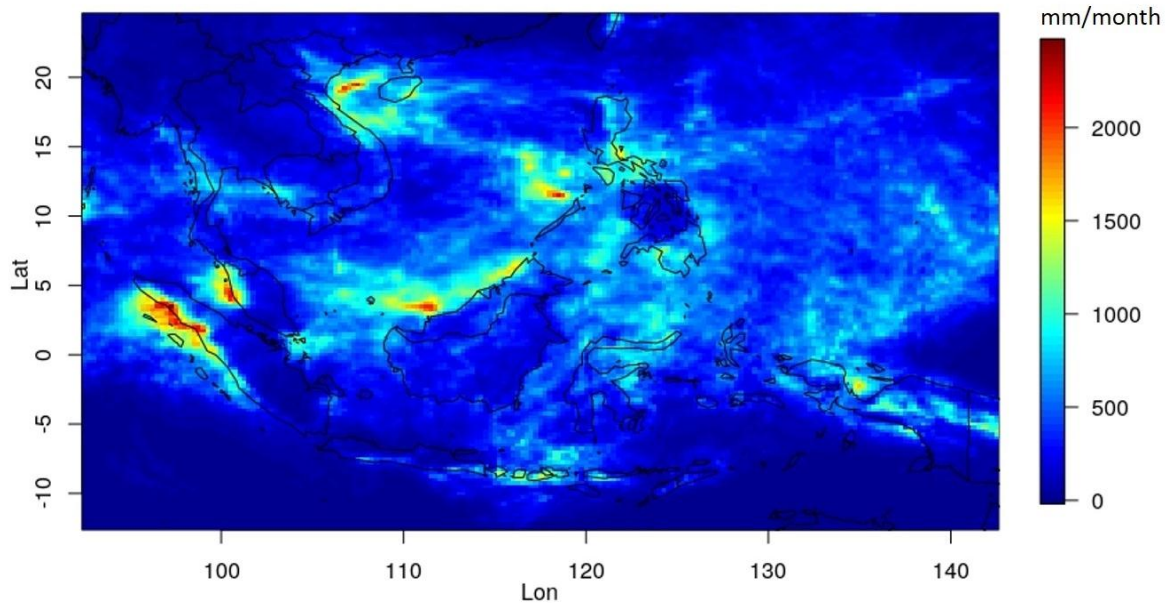
Figure 2. CORDEX-SEA domain (monthly precipitation) for October 2000

2.2.2 SA-OBS

SA-OBS is a daily high-resolution land-only observational gridded dataset for precipitation and minimum, mean and maximum temperature covering Southeast Asia region. This data set is delivered in 0.25◦ by 0.25◦ and a 0.5◦ by 0.5◦ regular latitude-longitude grid for the period of 1981–2016 (Van Den Besselaar et al., 2016). Observation data are collected under the Southeast Asian Climate Assessment & Dataset (SACA&D) which is a cooperation between *Badan Meteorologi klimatologi dan Geofisika* (BMKG) and meteorological services in the region. As the result of the cooperation, 1394 precipitation stations, 365 stations with minimum and maximum temperature, and 274 stations with daily mean temperature are selected. The SA-OBS is available based on kriging interpolation method using a geographically independent variogram as gridding method based on the one for the European gridded dataset E-OBS as described by Haylock et al. (2008).

2.2.3 Gap filling of SA-OBS

The SA-OBS was selected as observation data to bias correct the CORDEX-SEA. The result showed that there were some gap or empty cells for bias corrected results of temperature which is concentrated between longitude 155 to 130 (Figure 4). This is due to the missing value in gridded mean temperature of SA-OBS.

In order to fill the gap of the bias corrected results of temperature by SA-OBS, CRU TS v. 4.00 dataset was used. CRU TS v. 4.00 is one of the monthly temperature datasets developed by The Climatic

5

Research Unit. The Angular Distance Weighting (ADW) is used for gridding the monthly anomalies. The datasets cover the period of 1901-2015 for all land areas (excluding the Antarctica) at 0.5° resolution (Harris et al., 2014). In this research, CRU TS 0.5° resolution was re-gridded to 0.25° resolution of CORDEX-SEA datasets using the nearest neighbour method under climate data operators (CDO) command, explained by Schulzweida et al. (2006). Domain between longitude 112-140 and latitude 11 − 14 was used for the gap filling process (Figure 5).
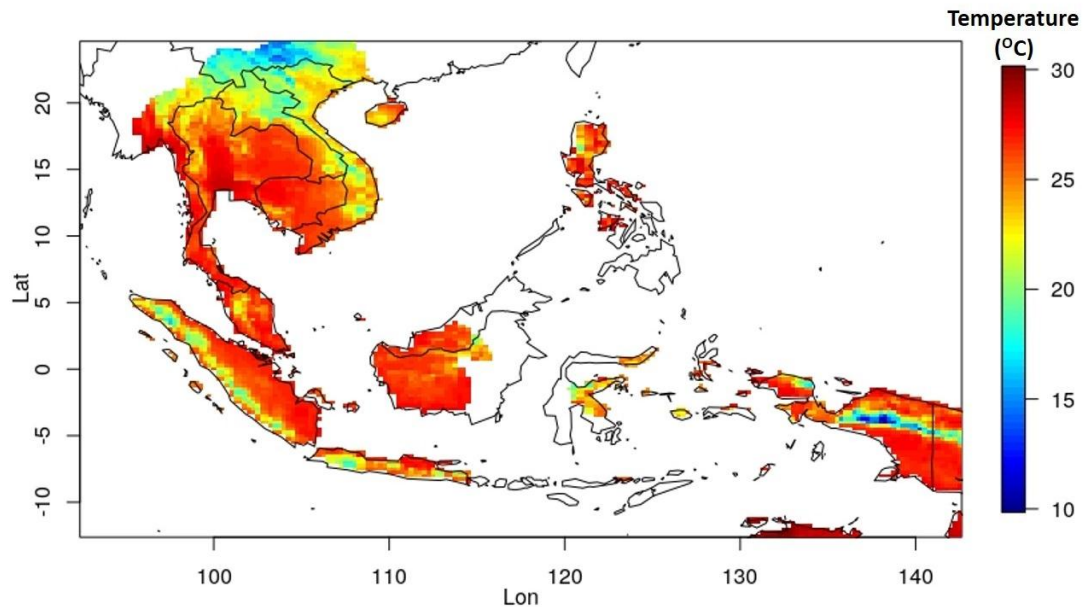
Figure 3. Monthly bias corrected temperature CORDEX-SEA by SA-OBS for October 2000.
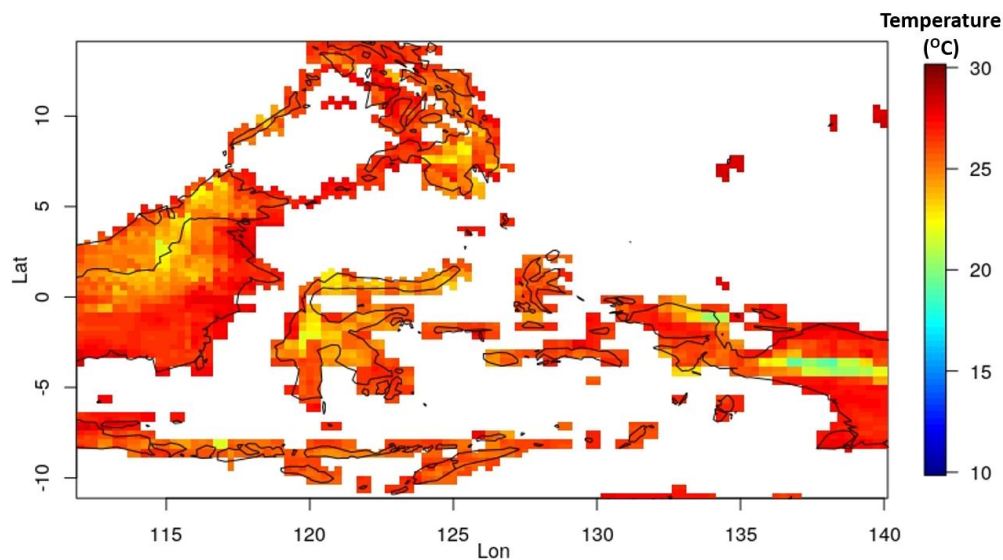
Figure 4. CRU TS domain for gap filling SA-OBS (longitude 112°-140° and latitude -11°− 14°). Monthly bias corrected temperature CORDEX-SEA by daily CRU for October 2000.

The bias correction process was run on a daily time scale, therefore daily temperature data must be constructed from monthly CRU dataset (Figure 6). This was done by calculating daily temperature anomaly from SA-OBS (Figure 7). Furthermore, the anomaly is added to monthly CRU gridded data to construct a daily gridded dataset, with an assumption that the daily anomaly and range data distribution within the domain are the same. This dataset is used to bias correct CORDEX-SEA data,

as the result, it filled the empty (missing value) grid cells in bias corrected CORDEX-SEA using SA-OBS (Figure 8). The performance of gap filling of constructed daily CRU is discussed in section 3.2.
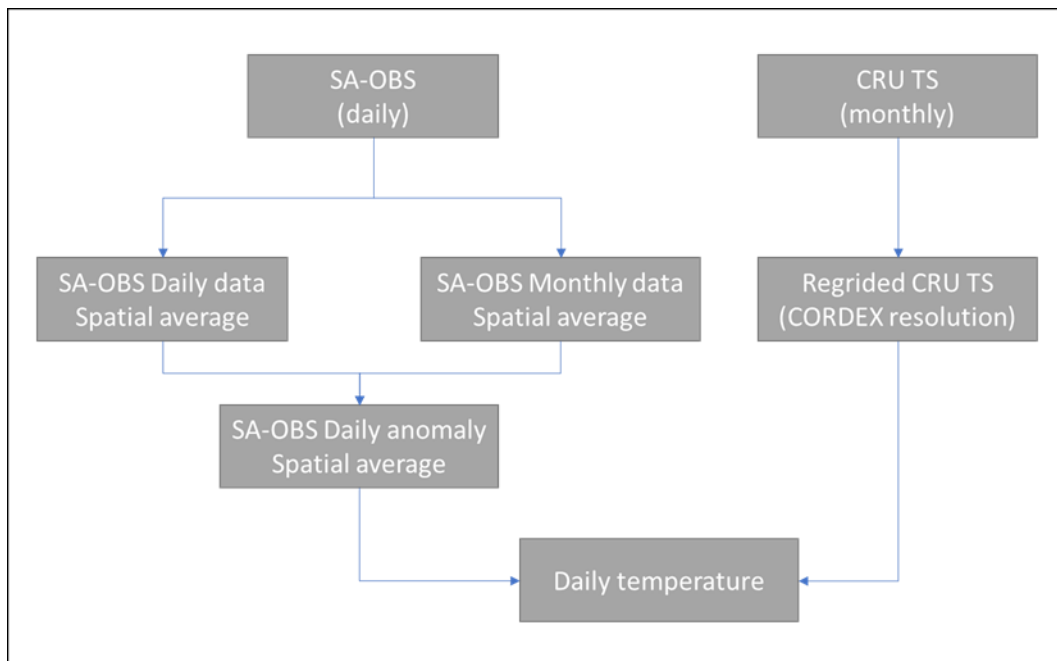

Figure 5. Construction of daily temperature from CRU monthly temperature
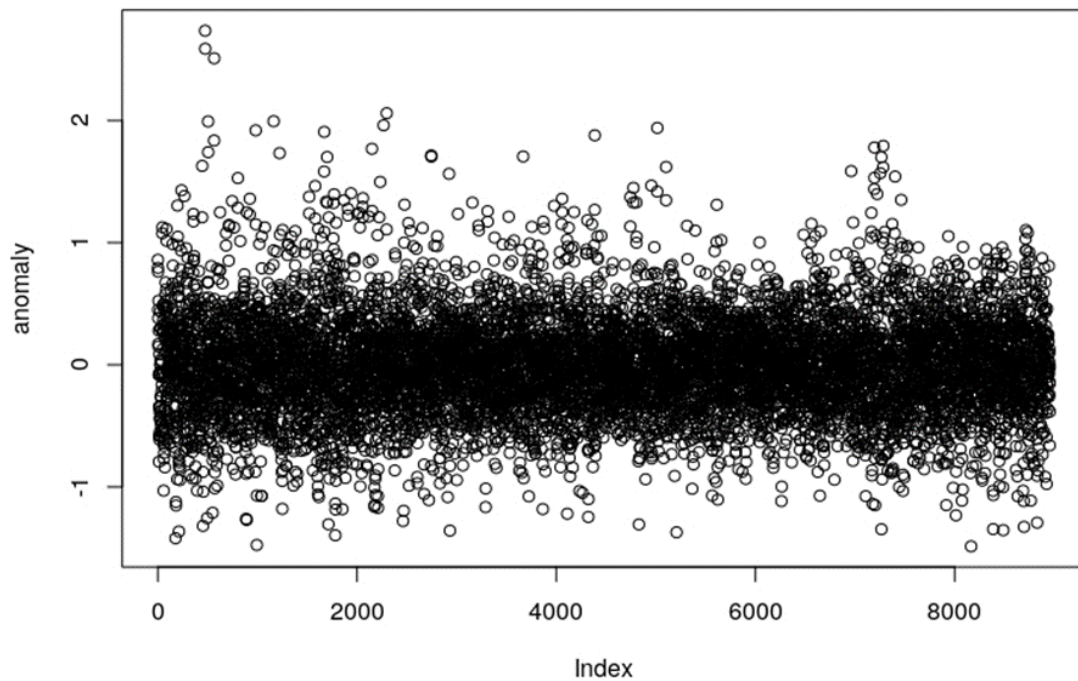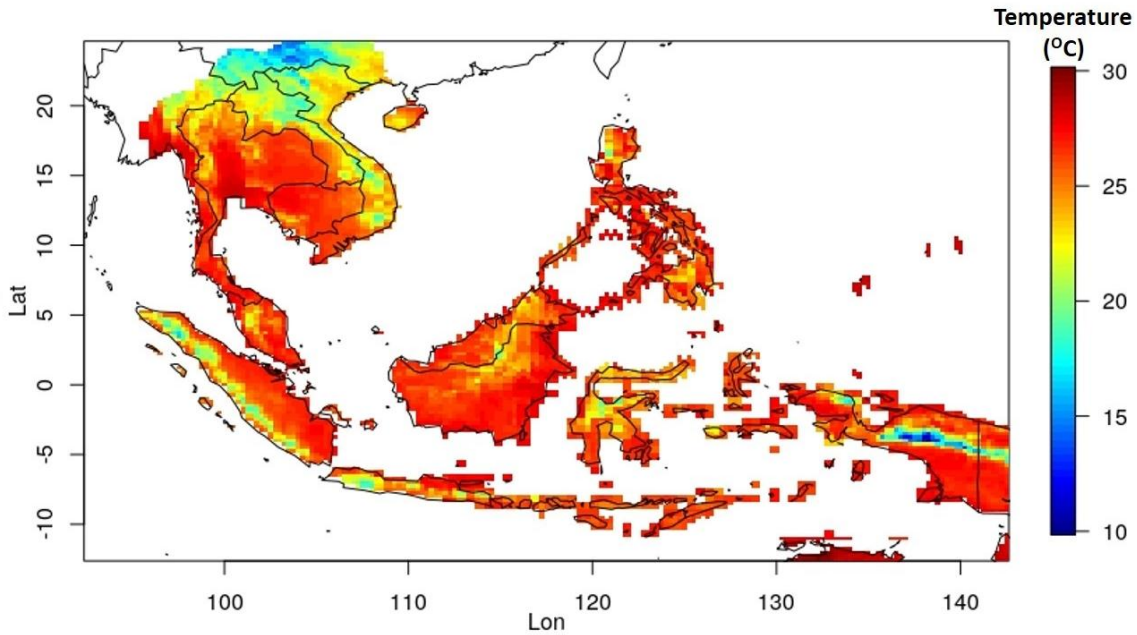

Figure 6. Spatial average of daily anomaly temperature

Figure 7. Example of gap filling result for monthly bias corrected temperature for October 2000.

To investigate performance of gap filling method on bias corrected temperature by constructed daily CRU (BC-CRU), there are 4 grid cells selected inside the gap filling domain. The data is compared to an uncorrected model (model) and bias corrected model by SA-OBS (BC-SAOBS). As expected, BC-SAOBS have a better performance than BC-CRU, this is because SA-OBS data was used as the observation data (Figure 9 & Table 2).

Overall, the BC-CRU improved the model data. This was shown by QQplot and ECDF value, which better fit to the SA-OBS, compared to the uncorrected model data (Figure 8 and Appendixes 1 & 2). Furthermore, the mean value of BC-CRU was closer to the SA-OBS, compared to model (Table 2). The construction of daily CRU data was made under the assumption that the domain has the same daily temperature anomaly. This was done by averaging the daily anomaly over the domain shown in figure 5 of SA-OBS data and adding it to the monthly CRU. The averaging made the anomaly of the domain relatively small. As a result, the standard deviation of BS-CRU was smaller than SA-OBS, model and BC-SAOBS. Based on the standard deviation, the model data has a closer standard deviation to the SA-OBS than BC-CRU (Table 2). Figure 12 show the verification plots for one grid cell, the figures of the other grid cells are shown in the appendix 5 (QQplot) and appendix 6 (ECDF).

Table 2. Mean and Standard deviation of (STDev) of temperature (°C) from SA-OBS, uncorrected model (model), bias corrected model by SA-OBS (BC-SAOBS) and bias corrected model by constructed daily CRU (BC-CRU)

| No	SA-OBS		Model		BC-SAOBS		BC CRU	
	Mean	STDev	Mean	STDev	Mean	STDev	Mean	STDev
1	25.419	0.824	22.028	0.822	25.419	0.823	25.317	0.570
2	24.678	1.416	26.407	0.950	24.678	1.416	25.649	0.679
3	23.805	1.491	26.195	0.916	23.805	1.490	25.597	0.639
4	23.731	1.608	27.631	0.740	23.731	1.607	25.597	0.639

8
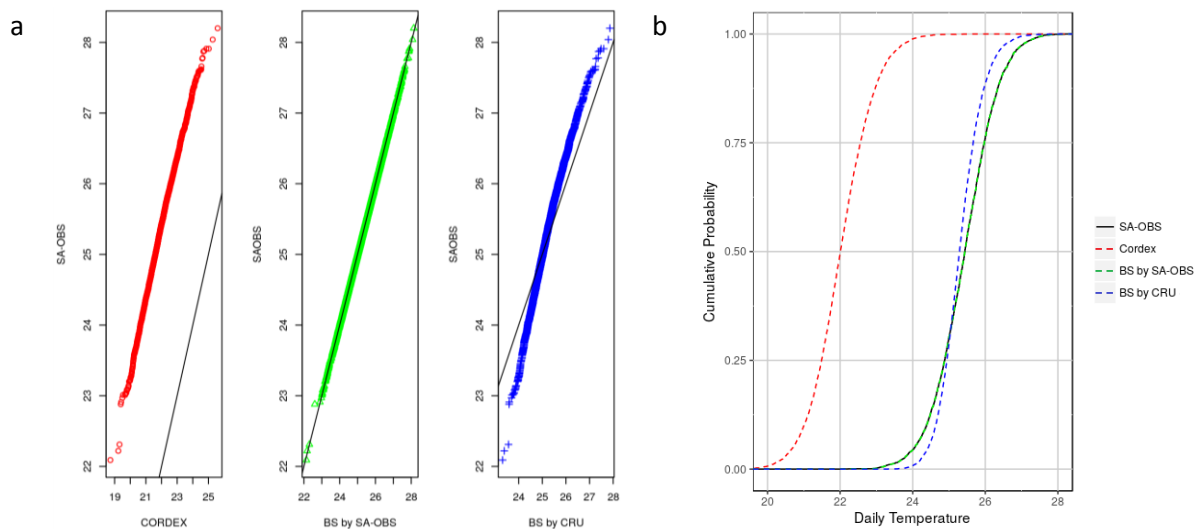
Figure 8. QQplot (a) and ECDF (b) of temperature of CORDEX-SEA raw data, bias corrected data by SA-OBS and bias corrected by constructed daily CRU. All data are compared to SA-OBS data.

2.2.4 Gridded harmonized soil datasets

The gridded harmonized soil dataset is a high resolution NETCDF file that describes global soil parameters from the Harmonized World Soil Database (HWSD) v1.2. There are four sources of database that were used to compile this database, namely, the European Soil Database (ESDB), the 1:1 million soil maps of China, various regional SOTER databases (SOTWIS Database), and the Soil Map of the World. The data were re-gridded and up-scaled from the Harmonized World Soil Database v1.2, including the area weighted soil organic carbon (kg C per m^2) and other parameters (Wieder et al., 2014). The most comprehensive database of soil characteristics that is a resource for evaluating soil biogeochemistry models is produced by FAO (2012). Soil characteristics in the HWSD represent data from real soil profiles at various stages of paedogenic development, land use, land use history, and disturbance history. It is available for surface soil horizons (0 to 30 cm) and deeper soil profiles (30 to 100 cm). This research used gridded available water content (AWC) data from this dataset which is available online from the Oak Ridge National Laboratory Distributed Active Archive Centre (http://daac. ornl. gov) (Figure 3).
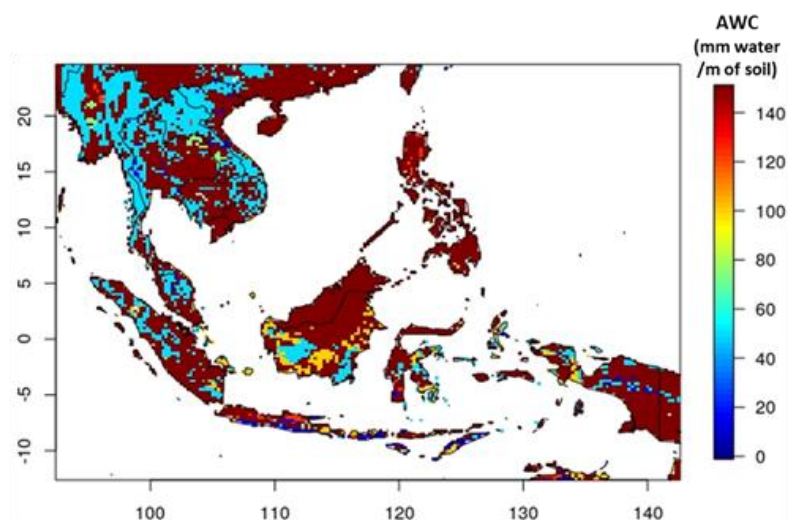
Figure 9. Regridded available water content (AWC) data (0.25^O resolution)

2.3 A self-calibration Palmer Drought Severity Index (scPDSI)

The scPDSI was introduced by Wells et al. (2004). It is an improvement of the original version of PDSI that was developed by Palmer (Palmer, 1965). In the original version, Palmer used weighting and calibration factors in his algorithm, empirically derived from data from the US Great Plains. Whereas the improved version (scPDSI) replaces the empirically derived climatic characteristic and duration factor that is used in original PDSI, with other values that are calculated from historical climate data specific for each location, to make results from different climate regimes more comparable (Wells et al., 2004; van der Schrier et al., 2006).

In the PDSI algorithm, four values relating to the soil moisture are computed together with their complementary potential values. This computation has monthly time steps. These values, including the complementary potential values, are evapotranspiration (ET), recharge (R), runoff (RO), loss (L), potential evapotranspiration (PET), potential recharge (PR), potential runoff (PRO), and potential loss (PL) (Palmer, 1965).

Furthermore, the 'Climatically Appropriate Conditions for Existing Conditions' (CAFEC) precipitation Ṕ is calculated, which represents the amount of rainfall that is required to maintain a normal soil moisture level for each month. The difference between the actual rainfall in a specific month and the computed CAFEC rainfall is the moisture departure.

The same moisture departure will have a different mean at different locations and times. To correct this problem, the moisture departure is weighted using a climatic characteristic value. The scPDSI version improves the climatic characteristic value by using factors from base period, in order to determine the representative climatic conditions. In addition, the calibration period is calculated to make the PDSI is comparable between diverse climatological regions. Furthermore, in this study, the base period and the calibration period are taken as the same.

Scaling is used in the scPDSI algorithm to make the scPDSI probability distribution roughly between -4 and +4. In order to make extreme drought in the future comparable to the one in historical times, we need to use the same scaling in all time periods. Therefore, data of historical and future periods under different RCP was combined for a one-time calculation (run), in order to maintain the probability distribution roughly between -4 and +4 for all periods (historical and future). This makes the result applicable for PDSI classification (Table 3). Using only historical period on the scaling, can make the scPDSI value in the far future period very high and may lead to this being only classified as extreme drought.

In addition, in this thesis, PET was derived from Thornthwaite's method (Thornthwaite, 1948), which requires temperature and latitude as an input. The method was constructed from the correlation between evapotranspiration with mean monthly temperature. It is developed from water balance for valleys in the eastern USA. To derive the potential value, sufficient moisture water was available to maintain active transpiration.

In Thornthwaite's method equation, heat index is calculated from temperature. Non-corrected PET is computed from heat index and temperature, with an adjustment being made for the number of daylight hours. The values are corrected by the real length of the month and the theoretical sunshine hours for the latitude of interest area. The Thornthwaite (1948) formula for monthly PET (mm) is:

$$PET = 16\, d\, (10\, T - I)^{\alpha}$$

Where T is the monthly mean temperature (in °C), I is the annual heat index which is the sum of monthly heat indices ($i = (T/5)^{1.514}$), d is a correction factor which depends on latitude and month, and α is calculated from the annual heat index ($0.49 + 0.0179\,I - 0.0000771\,I^2 + 0.000000675\,I^3$).

Table 3. The scPDSI classification

PDSI value	PDSI Category
Above 4.00	Extreme wet spell
3.00 − 3.99	Severe wet spell
2.00 − 2.99	Moderate wet spell
1.00 − 1.99	Mild wet spell
0.50 − 0.99	Incipient wet spell
0.49 to -0.49	Normal
-0.50 to -0.99	Incipient drought
-1.00 to -1.99	Mild drought
-2.00 to -2.99	Moderate drought
-3.00 to -3.99	Severe drought
Below -4.00	Extreme drought

3. RESULTS

The result in this report will be expressed in four main sections. The first section is about the results from the selection of bias correction methods (3.1). The second section regards the comparison between drought condition in EN 1982, 1997 and 2015 (3.2), followed by the result of drought severity change in the future under RCP4.5 and RCP8.5 (3.3).

The seasonal period of September-November (SON) was used in the analysis. The Nino3.4 index has the highest correlation with precipitation in the SON period (Figure 10). In Indonesia, the SON period is a very important season as it is the beginning of rainy season, when the growing season also starts. The highest loss of agriculture production in EN years is because of the late onset of the rainy season.
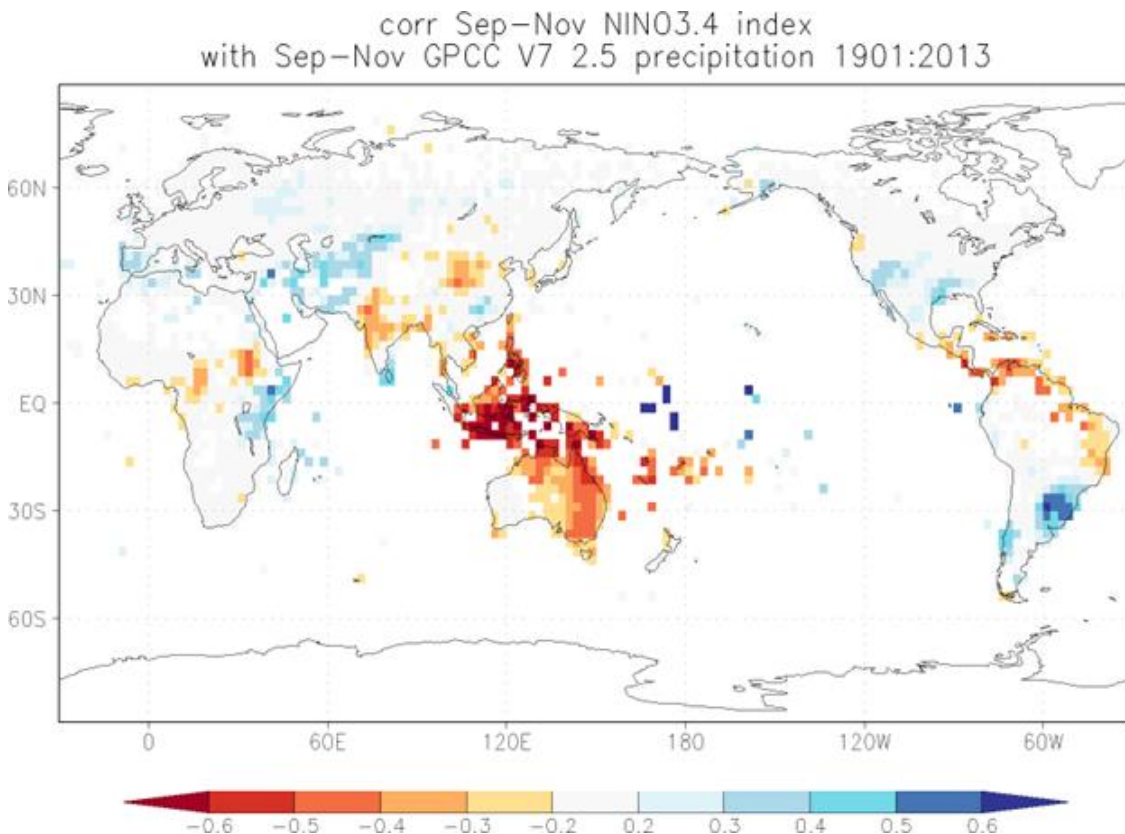
Figure 10. Correlation between Nino3.4 index and precipitation for September-November (SON) seasonal period (source: KNMI explorer)

3.1 Bias correction method selection

Three bias correction methods were compared in this study; eQM, gQM and scaling. The eQM and scaling methods were applied for precipitation and temperature. Meanwhile, gQM method was applied only for precipitation. Bias correction results are presented here using verification diagrams such as ECDF plot and QQ-plot, which present the performance of the methods. 10 grid cells and 6 grid cells were chosen in the selection of the best method of bias correction for precipitation and temperature respectively.

The eQM showed the best performance compared to other methods. The result is in accordance with the study performed by Pianiet al. (2010). For precipitation over all the grids that have been analysed, the QQplot plot showed that the CORDEX-SEA data, after the bias correction based on the

eQM, fitted better to the SA-OBS when compared to the other two models (Figure 11a and appendix 3). Corrected precipitation based on scaling and gQM methods still overestimated the observation. Similarly, this pattern was also found in ECDF, the result showed that the corrected precipitation using eQM fit very well to the SA-OBS, when compared to the other models (Figure 11b and appendix 3).

Furthermore, for temperature analysis over 6 grid cells, the corrected temperature based on the eQM method showed best performance compare to scaling and gQM. In the QQplot, corrected temperature using eQM fitted the SA-OBS (Figure 12a and appendix 5). In addition, the ECDF showed corrected temperature trend followed the SA-OBS cumulative probability (Figure 12b and appendix 5). The improvement after the bias correction was also shown on the scaling method, however there are still biases; underestimated the temperature below 26°C and overestimate the temperature above 26°C (Figure 12a and appendix 5). Figures 11 and 12 in this chapter show the verification plots in one grid, which contains the Dramaga and Bangkok stations. The figures of the other grids are shown in the appendixes.
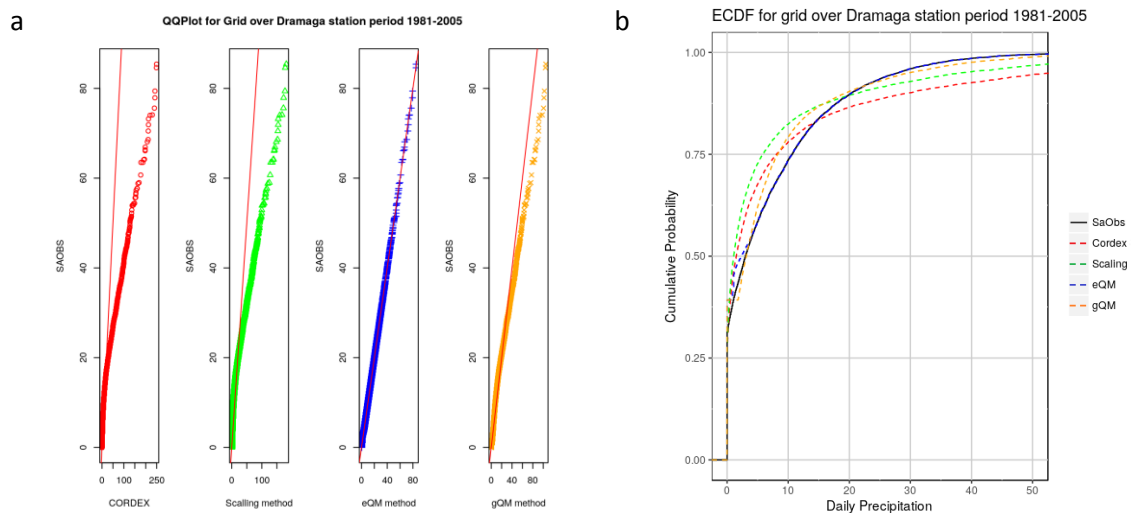

Figure 11. QQplot (a) and ECDF (b) QQplot of precipitation based on scaling (green), eQM (blue), and gQM (orange) methods for Dramaga station in the period of data 1981-2005.
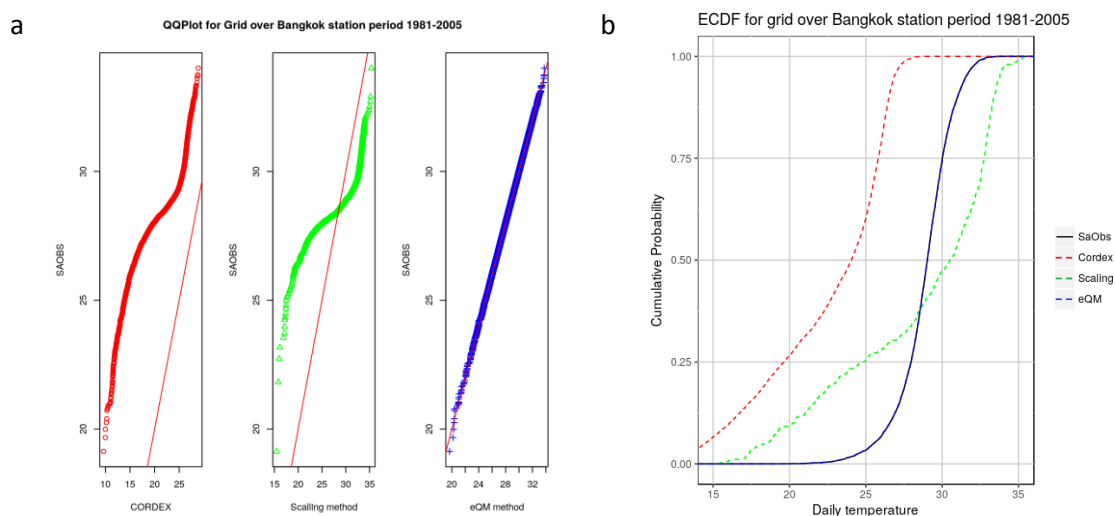
Figure 12. QQplot (a) and ECDF (b)of temperature based on scaling (green) and eQM (blue) methods for Bangkok station in the period of data 1981-2015.

3.2   Drought in different El-nino events

This section presents the result of *sc*PDSI calculation from SA-OBS precipitation and CRU temperature data. This result aims to answer the second research question: "*how is the condition of drought during EN 2015 compared to EN 1997 and EN 1982?*". EN 2015 was not classified as strong EN event like as EN 1982 and 1997. The precipitation anomaly for SON period in Southeast Asia region (SA-OBS dataset) showed that negative anomaly during EN 2015 is less when it was compared to EN 1997, although it is more when it was compared to EN 1982. But, less precipitation was not the only problem in EN 2015, it is also recorded by NASA that this year was the warmest year. This was showed by the temperature anomaly from CRU dataset that more than 40% of the region was experienced temperature more than 0.5^{O}C warmer compared to the average year. This was much warmer compared to temperature condition during EN 1982 and EN 1997 (Figure 13).
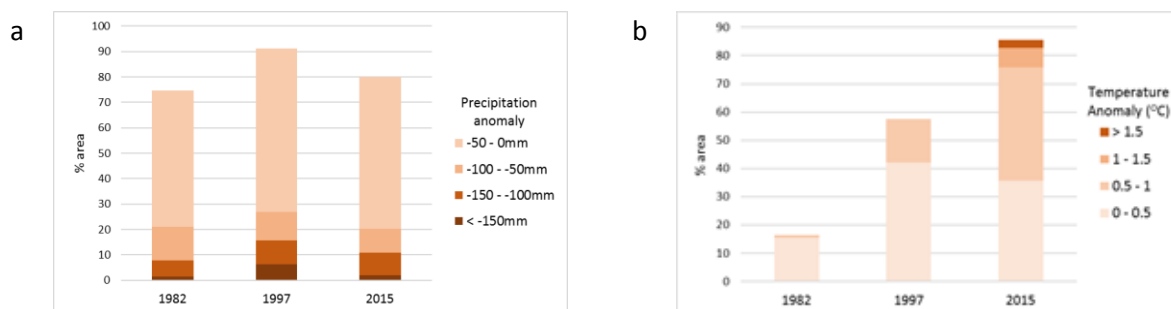
Figure 13. Percentage area of precipitation (a) and temperature (b) anomalies for EN 1982, 1997 and 2015

As a result of precipitation and temperature anomalies, drought in EN 2015 affected more areas compared to EN 1982 and EN 1997 even with more severe condition. Comparing EN 2015 to the other two EN events; total area affected by moderate to extreme drought in EN 2015 was slightly higher, although the percentage of area affected by extreme drought in EN 2015 was less (Figure 14).

In general, the spatial pattern of the three EN events was slightly different among each other. During EN 1997, drought was more concentrated in the north part of the region (Thailand, Cambodia, Laos, Malaysia and Philippine). Whilst, the spatial pattern of drought during EN 2015 was more similar to EN 1982 which more spread to Indonesian region (Figure 15).
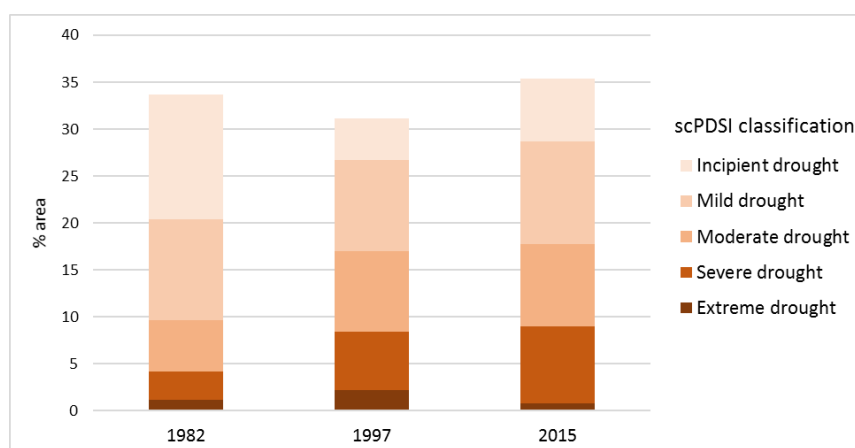
Figure 14. Percentage areas that affected by drought in 1982, 1997 and 2015
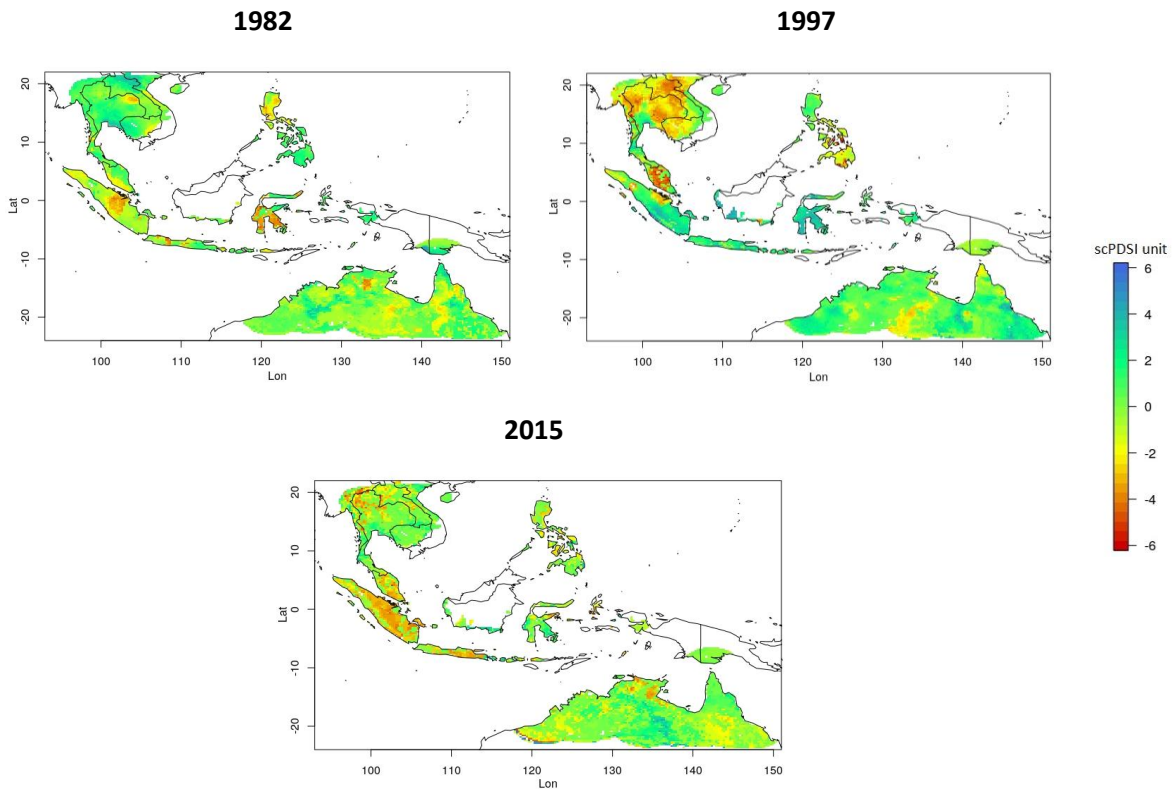
1982   **1997**

2015

Figure 15. The scPDSI in 1982, 1997 and 2015

3.3   Drought severity change projection

This section extends the results of the drought severity change in the near future period under RCP4.5 (NF-4.5), near future period under RCP8.5 (NF-8.5), far future period under RCP4.5 (FF-4.5) and far future period under RCP8.5 (FF-8.5). The climatology of scPDSI in historical, near future and far future periods under RCP4.5 and RPC8.5 have been discussed in the first part of this section (3.3.1). The results of this part are intended to answer the sub research question: "*how will severity and spatial extent of drought in Southeast Asia change in the future compared to the historical period?*". In this regard, 7 smaller domains were selected to give overview which areas that have higher drought severity change in the future. They are Sumatera domain (Sumatera and Malaysia peninsula), Borneo, Java, Sulawesi, Papua, North-SEA (Thailand, Cambodia, Laos and Vietnam) and Philippine (Figure 16).

Furthermore, the percentage of areas affected by moderate and higher droughts were calculated for every year of all period. Due to the lack of information regarding EN in the climate model data series, in this thesis EN 1997, as the strongest EN event, was represented by return period of 30 years (RP30) drought event. In addition, assuming that EN 1982 was the second strongest EN event, it was represented by return period 15 years (RP15) drought event. Based on the percentage of drought affected areas series, projection change of RP30 and RP15 in the future are discussed in the second part (3.3.2). This result is to answer the sub research question: "*how frequent will drought conditions, such as EN 1997 and EN 1982, occur in the future?*". To add more detailed information on the region the same 7 smaller domain was used to show the frequency of year in the future that extended the driest year in historical period based on percentage moderate-extreme drought and base on the spatial average of the index.
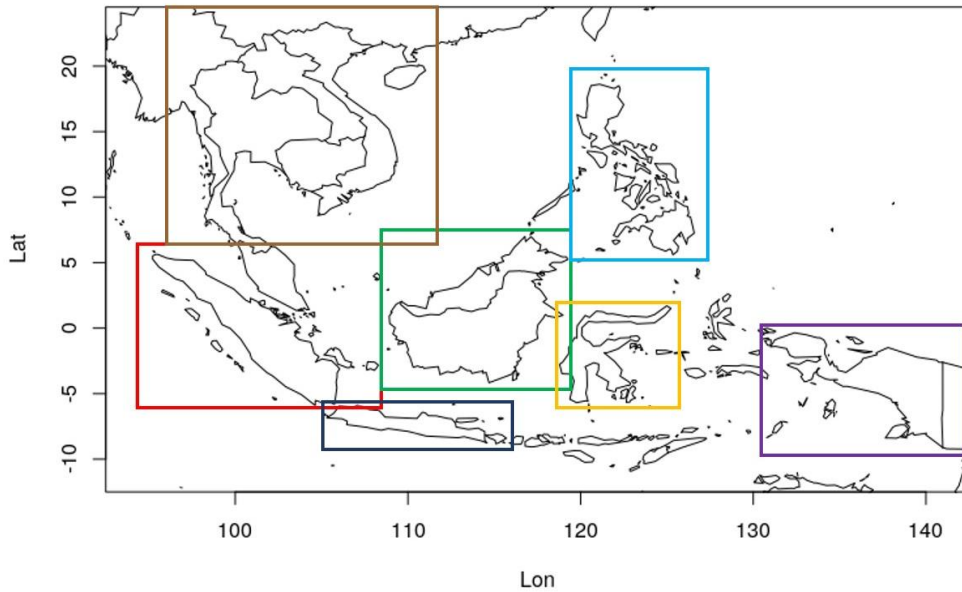
Figure 16. The selected 5 domains for local drought severity change analysis

Spatial condition of RP30 and RP15 in historical and future periods are discussed in the next part (3.3.3). The sub research question: "*how will severity and spatial extent of the drought of 30 years and 15 years return periods in Southeast Asia change in the future compared to a historical period?*" will be answered. Finally, the last part shows the outlook of precipitation and temperature projection under RCP4.5 and RCP8.5 (3.3.4).

3.3.1 Climatology of scPDSI in historical, near future and far future periods

In this sub section, the average condition of scPDSI for each period was calculated to describe the climatological condition of the period. The result showed that drought conditions are more likely to become more severe in the future. In historical period, most of the area is classified as mild drought, and only 4.5% of the region is classified suffering from drought conditions (below normal). Under both RCPs, the drought areas are projected to increase in the near future and even increase by even more in the far future period (Figure 17 and Appendix 8).
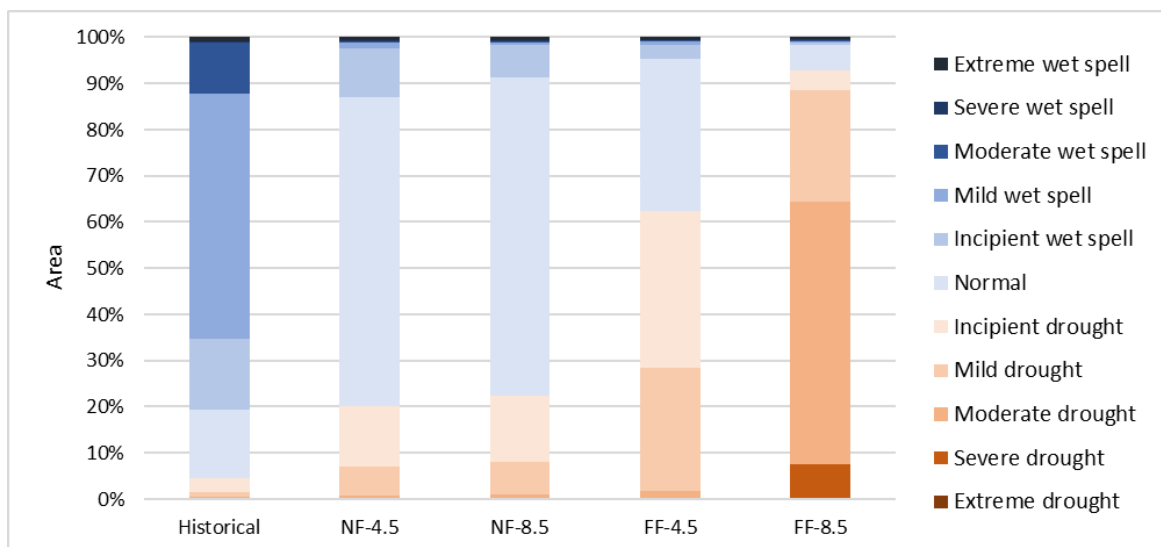
Figure 17. Percentage area of climatology of scPDSI

In near future period, conditions are similar in both RCPs scenarios. Areas affected by drought are projected to increase compared to historical period to slightly above 20%. Most of the area is still classified as normal condition (Figure 16). But, alarming condition will be appearing in the far future period. More than 50% of the area affected by drought in RCP4.5 scenario, with most of that area is classified as mild drought. Whilst in RCP8.5, disaster is inevitable with more than 90% area will be affected by drought, and most of that area is classified as moderate drought (Figure 17). The spatial distribution of climatology of scPDSI in historical and future periods are shown in appendix 8.

Some areas showed a high change of severity in the future. By calculating climatological and minimum values from spatial average of scPDSI for seven small domains (Figure 16), it is found that all domain over Indonesian regions (Sumatera, Borneo, Java, Sulawesi and Papua) have higher risk for drought condition compared to other regions (North-SEA and Philippine).

Table 4. Climatology (mean) and the driest conditions of 7 small domains

|		Historical	NF-4.5	NF-8.5	FF-4.5	FF-8.5
Sumatera	Mean	1.517	0.202	0.031	-0.993	-2.681
	Anomaly		**-1.315**	**-1.486**	**-2.510**	**-4.198**
	Driest	-0.415	-1.494	-1.481	-2.240	-3.943
	Driest Anomaly		**-1.079**	**-1.066**	**-1.825**	**-3.528**
Borneo	Mean	1.592	0.019	0.054	-0.732	-2.392
	Anomaly		**-1.573**	**-1.538**	**-2.324**	**-3.984**
	Driest	-0.869	-1.873	-1.703	-2.936	-4.737
	Driest Anomaly		**-1.004**	**-0.834**	**-2.067**	**-3.868**
Java	Mean	1.422	0.524	-0.352	-0.921	-2.779
	Anomaly		**-0.899**	**-1.774**	**-2.343**	**-4.201**
	Driest	-1.556	-2.384	-3.043	-3.519	-4.539
	Driest Anomaly		**-0.828**	**-1.487**	**-1.963**	**-2.983**
Sulawesi	Mean	1.392	0.033	-0.225	-0.776	-2.261
	Anomaly		**-1.360**	**-1.618**	**-2.169**	**-3.654**
	Driest	-0.810	-1.949	-2.401	-3.242	-4.791
	Driest Anomaly		**-1.139**	**-1.591**	**-2.432**	**-3.981**
Papua	Mean	1.475	0.093	-0.286	-0.743	-2.386
	Anomaly		**-1.382**	**-1.761**	**-2.218**	**-3.861**
	Driest	-0.376	-1.764	-1.838	-3.156	-4.473
	Driest Anomaly		**-1.389**	**-1.462**	**-2.780**	**-4.098**
North-SEA	Mean	0.876	-0.230	-0.033	-0.451	-1.590
	Anomaly		**-1.106**	**-0.909**	**-1.327**	**-2.466**
	Driest	-1.066	-1.710	-1.837	-3.405	-3.767
	Driest Anomaly		**-0.644**	**-0.771**	**-2.339**	**-2.701**
Philipine	Mean	0.084	-0.134	-0.979	-0.272	-1.603
	Anomaly		**-0.218**	**-1.063**	**-0.356**	**-1.687**
	Driest	-1.562	-1.845	-2.492	-2.124	-3.161
	Driest Anomaly		**-0.283**	**-0.930**	**-0.562**	**-1.599**

In near future period, all of the small domains have anomaly around -1 scPDSI unit value which mean that it will be classified 1 level drier than historical period, except for Philippine domain which has anomaly less than -0.3 scPDSI unit value. This condition tends to be more severe for domains over Indonesian region which has anomaly around -1.5 scPDSI unit value and can be classified as 2 levels drier than historical period (Table 4).

In far future period, almost two times drier condition compared to NF-4.5 appeared for FF-4.5. Whilst for FF-8.5, the condition of near future period almost nothing compared to it. The same pattern can still be found in far future period; North-SEA and Philippine domain have smaller anomaly compared to other regions in the equator. Especially, for Philippine domain, in RCP4.5, the condition in far future period almost similar with near future period, whilst for RCP8.5 in far future period the area will likely be classified 1 level drier compared to near future period (Table 4).

3.3.2   Projected change of 30 and 15 years return periods in the future

The analysis of return period change is based on the calculation of the percentage of areas affected by moderate and more severe drought in SON seasonal period. To get a better overview of the drought conditions in different periods, a series of the calculated percentage for every period are sorted. The year with the highest percentage of moderate-extreme drought area in the historical period is selected as the threshold condition for RP30, which represent the EN 1997, whereas the second highest percentage is selected as the threshold condition for RP15, which represents the EN 1982. Furthermore, frequency and return period change in the future were calculated to analyse how frequent the EN 1997 and EN 1982 drought conditions will occur in the future.

It is expected that with projected higher temperatures in the future, drought conditions in the future will be more severe. In the historical period, the percentage of moderate-extreme drought area was 0.8-15% of the region. It has been identified that the threshold for RP30 and RP15 is 15% and 12.5% respectively. In the near future period, the percentage of moderate-extreme drought area increased to 2.5-38.4% for NF-4.5 and 3.4-31,7% for NF-8.5 of the region. The percentage of the area increased more in the far future period, as it reaches 5.1-70.8% for NF-4.5 and 26.6-88.8% for NF8.5 (Figure 18).
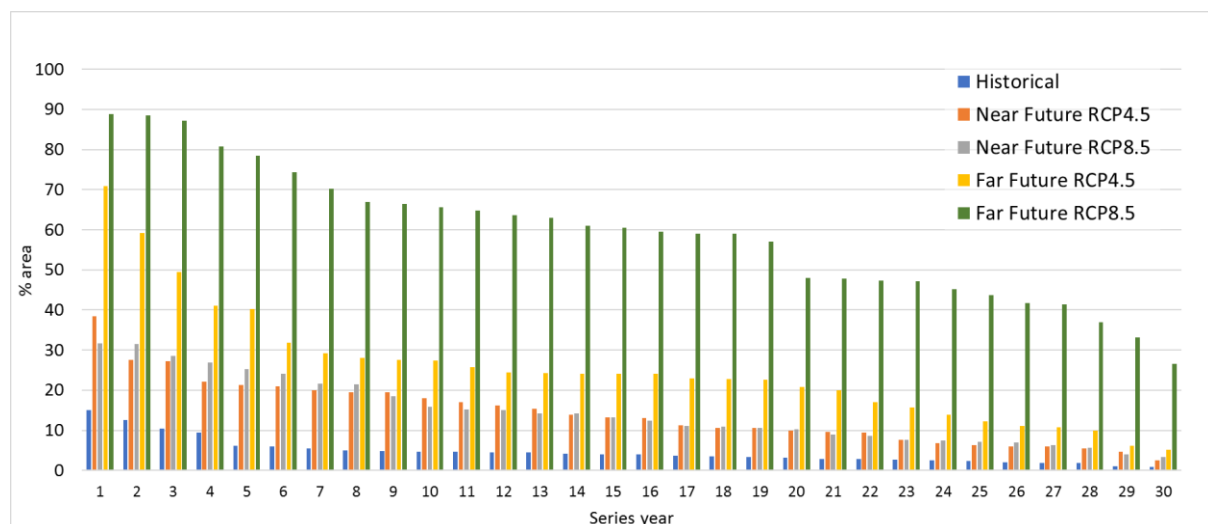
Figure 18. Sorted percentage area that classified as moderate, severe and extreme drought in historical and future periods

In the most extreme year of the historical period, the area percentage of moderate to extreme drought is still much less than the least drought years of the FF-8.5 (Figure 18). As the result, the

condition of EN 1997 which is represented by RP30 will occur every 3 years in the near future period, under both of the RCP scenarios. Furthermore, these conditions will be common in the far future. In addition, more frequent than EN 1997, the conditions of EN 1982 which are represented by RP15, will occur every 2 years in near future period, under both of RCP scenarios (Table 5).

Table 5. The return period 30 and 15 years change in the future

Return Period		Near future		Far future	
		RCP4.5	RCP8.5	RCP4.5	RCP8.5
30 years	Frequency	13	11	23	30
	Return Period	2.3	2.7	1.3	1.0
15 years	Frequency	16	15	24	30
	Return Period	1.9	2.0	1.3	1.0

Table 6 shows the frequency of year in the future that extended the driest year in historical period calculated from spatial average of scPDSI index value and percentage of moderate-extreme drought area for seven small domains to give overview which areas that have higher return period change in the future. The spatial average of scPDSI was calculated for small domain analysis because it is expected that in small domains the condition will be more uniform compared to the large domain (Southeast Asia domain). This can be shown by the frequency calculated by both method which has almost similar results. Except for North-SEA domain which has frequency from spatial average far lower compare to frequency from percentage drought area. This is due to the areas in the north part of North-SEA which tend to be wetter in the future. This condition is extreme different with other part of North-SEA which is drier in the future.

Table 6. The frequency of year in the future that extended the driest year in historical period calculated from spatial average of scPDSI index value and percentage of moderate-extreme drought area for seven small domains.

		NF-4.5	NF-8.5	FF-4.5	FF-8.5
Sumatera	Average	8	13	22	30
	Percentage area	7	5	18	30
Borneo	Average	6	7	14	27
	Percentage area	9	7	18	29
Java	Average	4	6	10	27
	Percentage area	4	6	11	27
Sulawesi	Average	12	10	17	26
	Percentage area	12	10	19	28
Papua	Average	13	14	19	29
	Percentage area	16	16	24	30
North-SEA	Average	2	5	7	20
	Percentage area	7	6	14	28
Philippine	Average	1	4	4	15
	Percentage area	2	6	4	20

In general, the result shows that domains over Indonesia region has more return period change in the future compared to other domains (North-SEA and Philippine). Especially for Sulawesi and Papua domains which already will experience the RP30 of historical period in every 3 years (frequency 10) in near future period under both RCP's.

3.3.3 Drought conditions of return period of 30 and 15 years in historical near future and far future periods

In this subsection, the series of percentage moderate-extreme drought area were used to identify the RP30 and RP15 years in historical and future periods. Furthermore, the selected year was displayed to compare the area and severity between historical and future periods under for RP30 and RP15.

A similar spatial pattern of drought area for RP30 year in the near future period under both RCP's and historical period was found. Drought area in RP30 historical period is concentrated over the north and the south part of Vietnam, the south part of Sulawesi and Borneo, the centre part of Java, Sulawesi and Papua. This concentrated area is larger, with more severe conditions, in near future condition. Both in NF-4.5 and NF-8.5, the drought area in the southern part of Vietnam spread to Cambodia and the southern part of Thailand. Similar things happen for the drought area in the southern part of Sumatera and Borneo. In Java, the drought area spreads more to all parts of the island. Whilst in Papua, more extreme drought severity was shown, especially for NF-8.5 (Figures 19, 20a and 20b). As a result, the percentage drought area of RP30 is higher in near future period with 76.4% for NF-4.5 and 68.4% for NF8.5, compared to 61.6% in historical period (Figure 21).
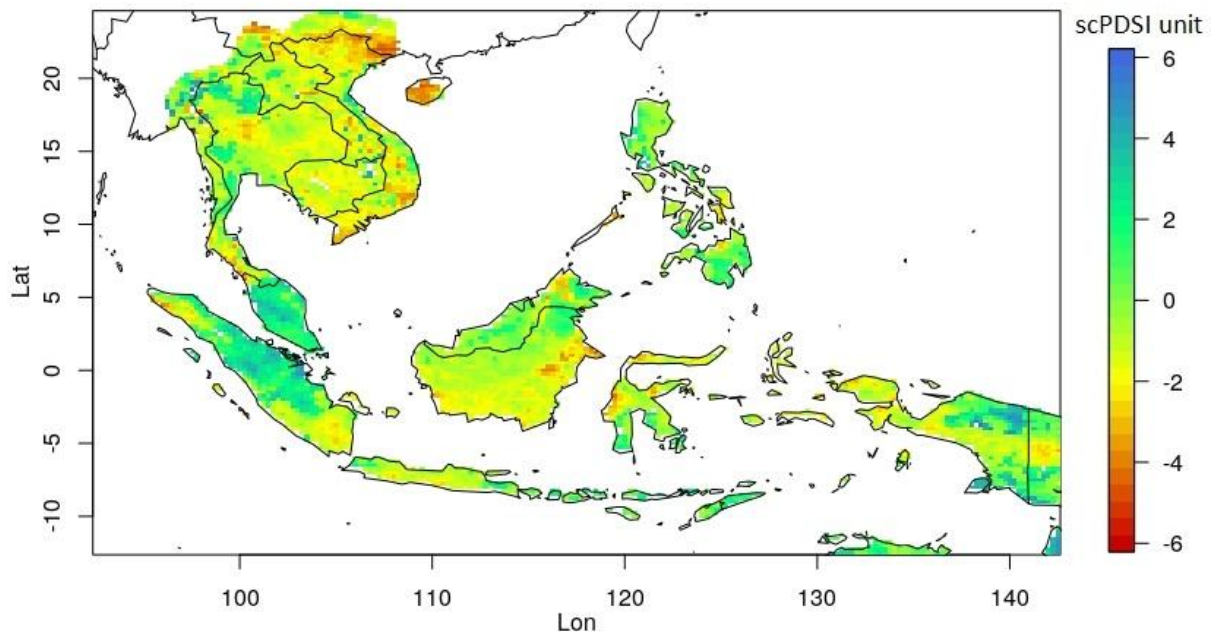

Figure 19. The drought condition in return period of 30 years for historical period in the model
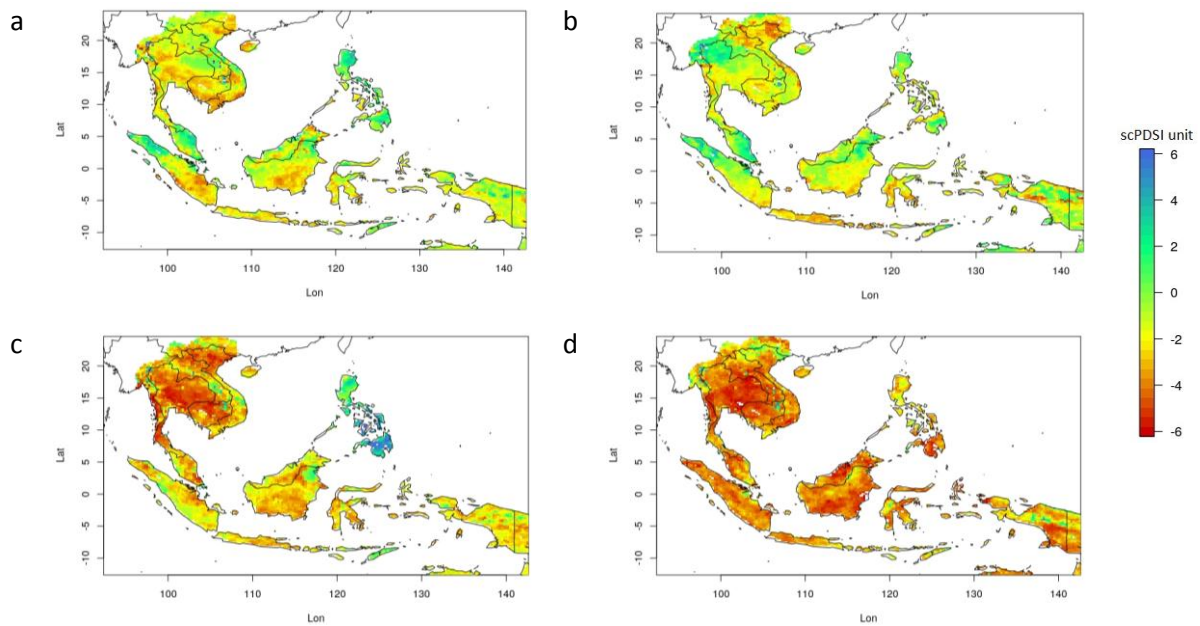
Figure 20. The drought condition in return period of 30 years for future period. Near future period for RCP4.5 (a) and RCP8.5 (b). Far future period RCP4.5 (c) and RCP8.5 (d).

More severe conditions are found in RP30 FF-4.5. Moderate to extreme drought conditions are found in almost every part of Thailand and Cambodia. The extreme drought was also found in the northern part of Vietnam and some parts of Malaysia. For Indonesia region, drought affected almost every part of the region. Contrast conditions are shown over the Philippine region, which has wet conditions (Figure 20c). The drought affects 87.4% of the areas of the region, where the remaining areas are still in normal and wet condition, but more concentrated in the Philippine region (Figure 21).
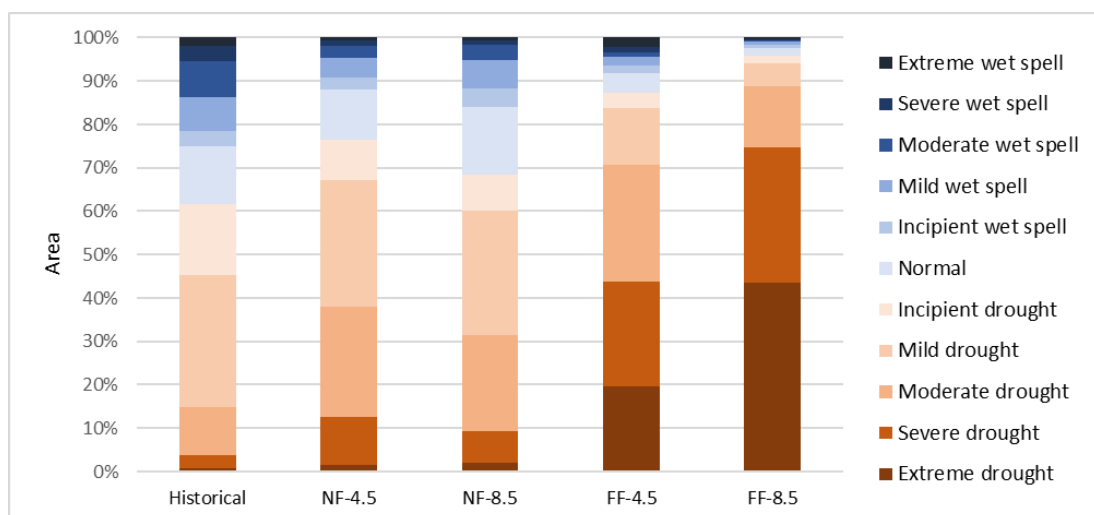
Figure 21. The percentage area of scPDSI index for RP30.

Horrifying conditions were found in RP30 FF-8.5. 43.6% of the region are affected by extreme drought. In addition, 31.0% and 14.1% of the areas are affected by severe and moderate drought. In total, 95.8% of the region are affected by drought, which leaves less than 5% areas that are not under drought conditions (Figure 20d & 21).

21

There was a slightly different spatial pattern found in RP15 and RP30 of historical and near future periods. Drought in RP15 for both periods are more concentrated in the Northern part of Vietnam and Laos (Figures 22, 23a and 23b). There are some severe drought conditions in the eastern part of Sumatera, the northern part of Borneo and the southern part of Papua in NF-4.5, but this condition is not shown in NF-8.5 (Figures 23a and 23b). The percentage of drought areas in historical period is 39.6%, the areas increased in near future period up to 60.5% for NF-4.5 and 64.7% for NF-8.5 (Figure 24).
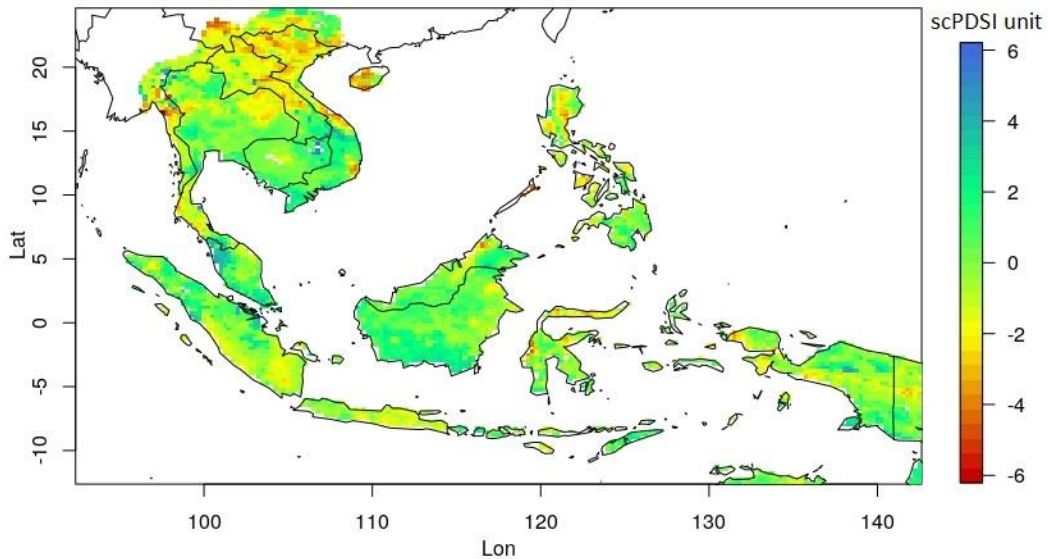
Figure 22. The drought condition in return period of 15 years for historical period in the model
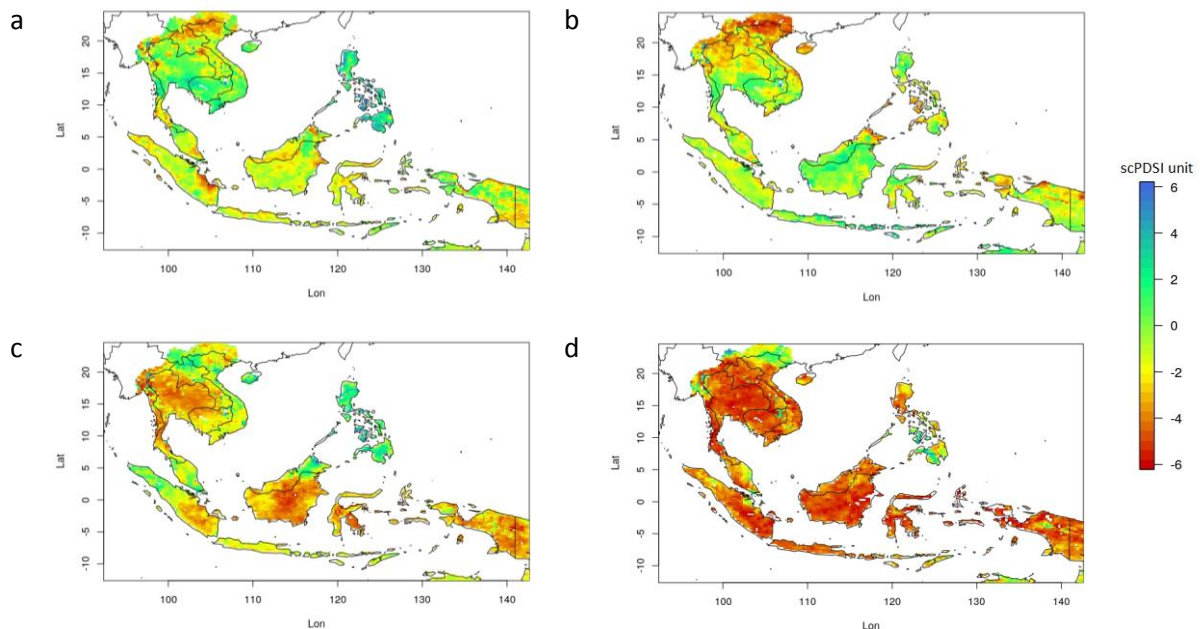
Figure 23. The drought condition in return period of 15 years for future period. Near future period for RCP4.5 (a) and RCP8.5 (b). Far future period RCP4.5 (c) and RCP8.5 (d).

In RP15 FF-4.5, severe drought affects Thailand, half of the south of Sumatera and most areas of Borneo, Sulawesi and Papua (Figure 23c). Furthermore, extreme conditions occur for FF-8.5, where extreme drought conditions have spread all over the region (Figure 23d). Unexpected result showed for FF-8.5, the areas that are affected by extreme drought in RP15 (64.4%) are larger than in RP30

(43.6%). This is because the criteria were based on total percentage areas affected by moderate-extreme drought which in this case in RP15 (88.4%) are slightly less than in RP30 (88.9%) (Figure 21 and 24).
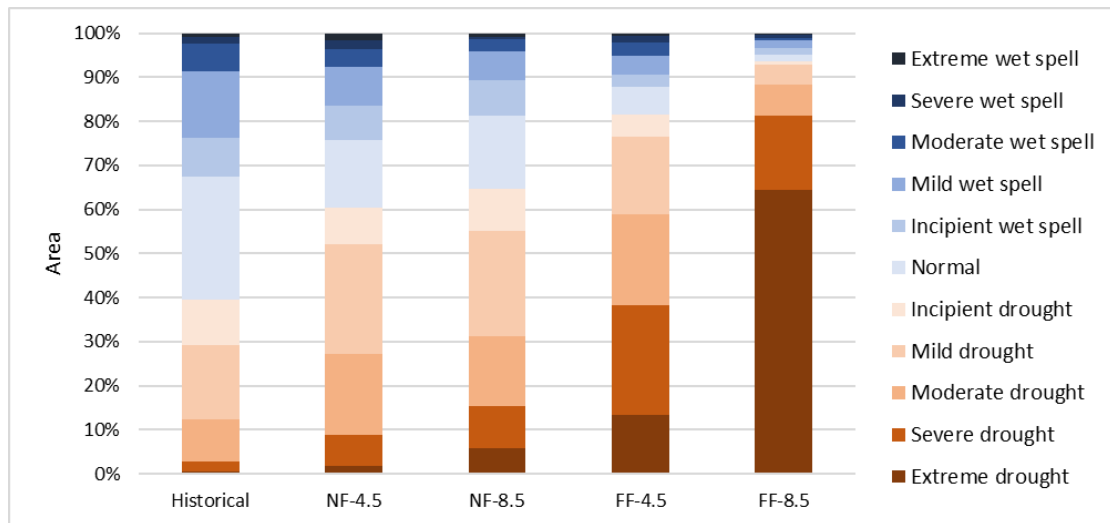
Figure 24. The percentage area of scPDSI index for RP15.

3.3.4 Outlook: Precipitation and temperature projections

This sub chapter discuss precipitation and temperature projection from RCM that is used in this analysis The aim is to find out whether the reported change in drought are primarily a temperature or primarily a precipitation effect. The CORDEX-SEA 25 Km from APCC is a model data that is used in this thesis. The model data employed HadGEM2-AO for the future projection. The HadGEM2-AO projected relative decreasing of precipitation in subtropical regions and increasing in tropical regions and at high latitudes. Especially for East Asia regions, the increasing precipitation is greater in summer (July-August) and less or even decreases in any other season (Baek et al., 2013). The data shows that in Southeast Asia regions, SON precipitation increases for all future periods and scenarios in some areas like Vietnam. However, for Sumatera and Borneo, precipitation decreases for all future period and scenarios (Figure 25).

In the RCP4.5 scenario, the anomaly of SON precipitation shows almost the same percentage areas with negative and positive anomaly (Figure 26). Most of the areas have precipitation decreasing precipitation less than 25mm/3months. The percentage areas with higher decreasing precipitation is more in the far future period. The highest negative anomaly was occurring for FF-8.5, but the anomaly is still relatively small for 3 months period. Especially with the fact that there still some areas with positive anomaly.

In contrast with precipitation projection, temperature projection shows relatively high anomaly in the future (Figure 27). In the near future period, still more than half of the area has anomaly below $1^{\circ}C$. Unexpected result shows for this period, percentage area with anomaly higher than $1^{\circ}C$ under RCP8.5 is lower than under RCP4.5. This lead to almost similar drought climatological condition of drought in NF-8.5 and NF-4.5 (Figure 17). Instead, NF-8.5 has less severity compared to NN-4.5 for RP30 (Figures 20 and 21). However, it should be noted that the relatively low increase of temperature for NN-8.5 was mentioned before is only for Southeast Asia region in SON seasonal period, which does not represent a global and climatological scale. Furthermore, the RP30 condition

was analysed from a selected one year that has the largest moderate-extreme drought area, which does not represent the climatological condition of the future period and scenario.

In general, the projection shows low anomaly of precipitation with high increasing trend of temperature in the future. It can be concluded that the increasing of spatial area and severity of drought for the future in the result of previous sections, it is more as an impact of the increasing trend of temperature than precipitation anomaly.
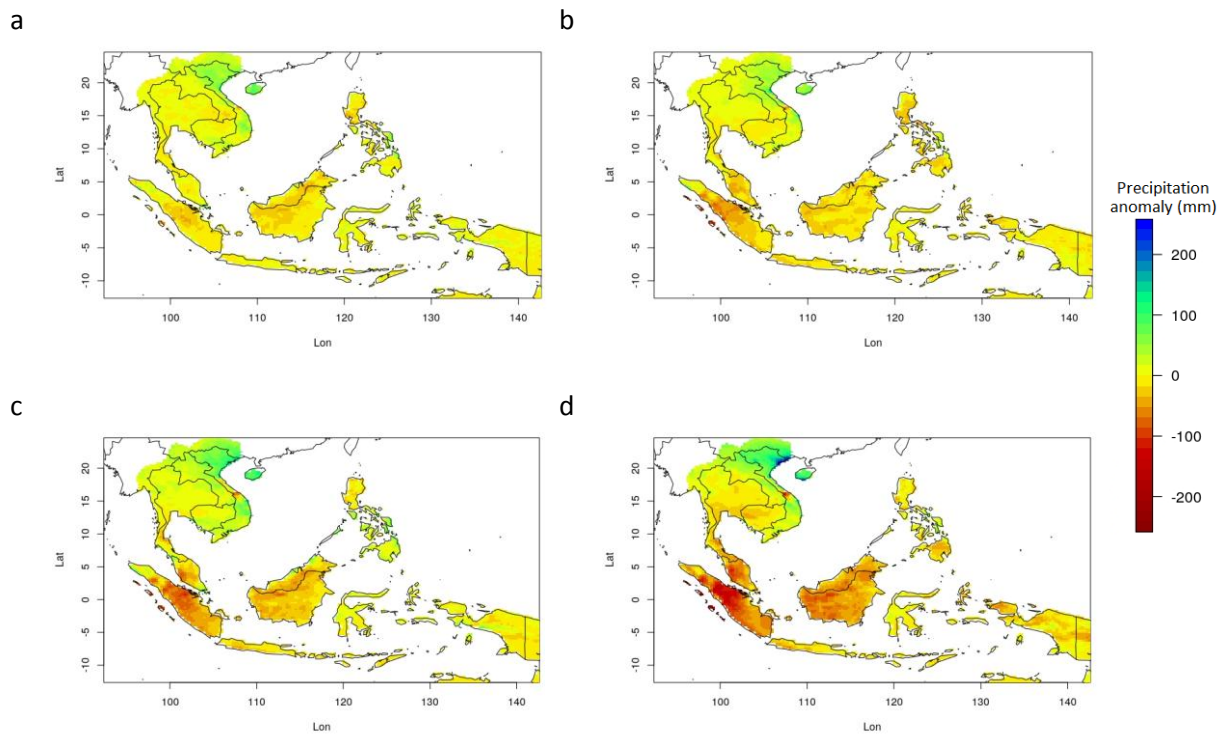
Figure 25. Precipitation (mm) anomaly for SON in the future period. Near future period for RCP4.5 (a) and RCP8.5 (b). Far future period RCP4.5 (c) and RCP8.5 (d).
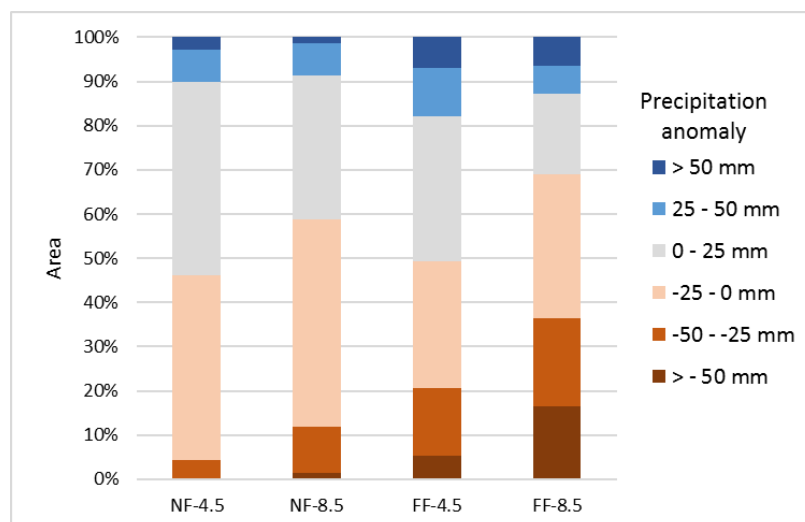
Figure 26. Percentage area of anomaly SON precipitation (mm) in the future.
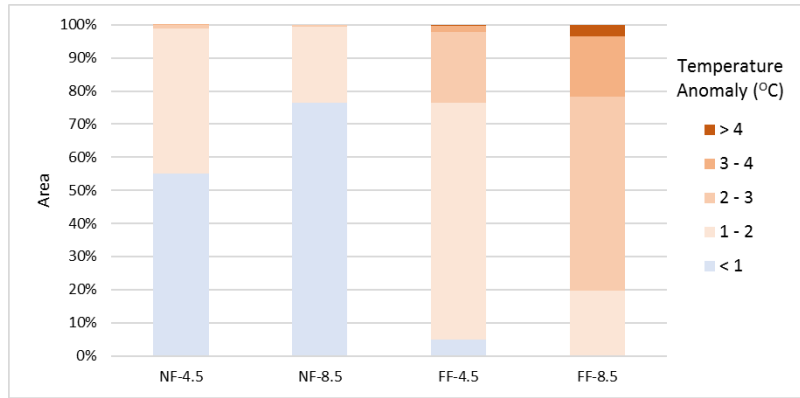
Figure 27. Percentage area of anomaly SON temperature (^{O}C) in the future.

4. DISCUSSION AND RECOMMENDATION

This section discusses the source of uncertainties related with data and approach of the thesis. The first uncertainty comes from RCM data set. Global Circulation models (GCM) produce different projection about climate variable conditions in the future. The output differences between GCMs is due to the way they parameterise different variables in their model. It is important to use different ranges of RCM for future projections. With only relying on one RCM, it may hide the range of uncertainty from the model projection differences. Due to the availability data, this thesis used only one model data for the future projections. The model output difference is one of the uncertainties in this thesis. For further research, it will be better to include as much model data as possible for future projection analysis, to show ranges of uncertainty from the model output in the information, which will be useful for a robust adaptation plan. This analysis can be done when the data are released from the CORDEX experiments.

The other uncertainty is in the calculation method for potential evapotranspiration (PET). In this thesis, PET was calculated from temperature and latitude using the Thornthwaite method (Thornthwaite, 1948)). PET is more sensitive to radiation, wind speed and relative humidity than to mean temperature (Gao et al, 2006). The standard method that is suggested by The United Nations Food and Agriculture Organization (FAO) was the Penman–Monteith equation (Monteith, 1965). Beside mean daily temperature, the method requires wind speed, relative humidity and solar radiation which seldom available in spatial scale.

PET estimation based on mean temperature cannot be relied on to estimate PET for short periods, but it can be used with low sensitivity for long periods, such as seasonal and annual periods (Pelton et al, 1960). In this thesis PET was calculated from temperature using Thornthwaite method for scPDSI index which in monthly time scale and analysed in 3 months seasonal period (SON).

The PET estimation by Thornthwaite method is tended to make the scPDSI value more sensitive to temperature anomaly, because temperature is the only climate variable that used in the estimation. It may lead to overestimating drought severity in future projection analysis. For further research, the Penman–Monteith equation (Monteith, 1965) is the most recommended option for PET estimation. Otherwise, using other methods that add radiation as an input, will improve the estimation.

5. SUMMARY AND CONCLUSIONS

In this study, we used scPDSI index to investigate drought conditions in different El-Nino years and different future periods under RCP4.5 and RCP8.5. The method was chosen because it is not only considering precipitation as the main factor, but also includes temperature in the calculation. In addition, empirical quantile mapping (eQM) method was used for bias corrected CORDEX-SEA data. The method performed better compared to scaling and gamma quantile mapping (gQM) for bias corrected RCM data in Southeast Asia region. This is the answer for the first research question.

The second research question was answered by calculating the scPDSI index from SA-OBS precipitation and CRU TS4 temperature data. The result showed that although EN 2015 has less precipitation anomaly compared to EN 1997 but the extreme temperature condition during that year could lead to more severe condition and more area affected by drought in the region.

To answer the other research questions related to future projection, scPDSI index was calculated from bias corrected CORDEX-SEA data. The result showed that in climatic condition drought affected areas increase around 15% in the near future period under medium (RCP4.5) and extreme (RCP8.5) climate change compare to historical period. Whereas in far future period, the area will increase more than 50%. Disaster is inevitable under extreme climate change with almost the entire area will be affected by drought. In addition, the drought condition of RP30 and RP15 in historical period will consider nothing compare to the extreme condition in far future period.

Furthermore, related to return period change, drought as EN 1997 can be appear every 2-3 years under both RCP's in near future period. Also, we show that such droughts will be common in the far future period.

Based on analysis of small domains in the region, areas in the equatorial region such as Indonesia will have higher severity change and spatial extended of drought in the future compare to other areas in the Southeast Asia.

To conclude, although with a small rainfall anomaly, the increasing trend of temperature will increase the area and the severity of drought in the future. However, more model output data for future projection is needed to include the range of model uncertainty in the information, which is important for a robust adaptation plan.

REFERENCES

Baek, H. J., Lee, J., Lee, H. S., Hyun, Y. K., Cho, C., Kwon, W. T., ... & Lee, J. (2013). Climate change in the 21st century simulated by HadGEM2-AO under representative concentration pathways. Asia-Pacific Journal of Atmospheric Sciences, 49(5), 603-618.

Fang, G., Yang, J., Chen, Y. N., & Zammit, C. (2015). Comparing bias correction methods in downscaling meteorological variables for a hydrologic impact study in an arid area in China. Hydrology and Earth System Sciences, 19(6), 2547-2559.

Gao, G., Chen, D., Ren, G., Chen, Y., & Liao, Y. (2006). Spatial and temporal variations and controlling factors of potential evapotranspiration in China: 1956–2000. Journal of Geographical Sciences, 16(1), 3-12.

Gudmundsson, L., Bremnes, J. B., Haugen, J. E., and EngenSkaugen (2012), T.: Technical Note: Downscaling RCM precipitation to the station scale using statistical transformations – a comparison of methods, Hydrol. Earth Syst. Sci., 16, 3383–3390, doi:10.5194/hess-16-3383-2012.

Harris, I. P. D. J., Jones, P. D., Osborn, T. J., & Lister, D. H. (2014). Updated high-resolution grids of monthly climatic observations–the CRU TS3. 10 Dataset. International Journal of Climatology, 34(3), 623-642.

Haylock, M. R., Hofstra, N., Klein Tank, A. M. G., Klok, E. J., Jones, P. D., & New, M. (2008). A European daily high-resolution gridded data set of surface temperature and precipitation for 1950–2006. Journal of Geophysical Research: Atmospheres, 113(D20).

IPCC (2014). Climate Change 2014–Impacts, Adaptation and Vulnerability: Regional Aspects. Cambridge University Press, 2014.

Jiménez-Muñoz, J. C., Mattar, C., Barichivich, J., Santamaría-Artigas, A., Takahashi, K., Malhi, Y., ... & van der Schrier, G. (2016). Record-breaking warming and extreme drought in the Amazon rainforest during the course of El Niño 2015–2016. Scientific Reports, 6.

Kirono, D. G., Tapper, N. J., & McBride, J. L. (1999). Documenting Indonesian rainfall in the 1997/1998 El Nino event. Physical Geography, 20(5), 422-435.

Ministry of Agriculture (2016). BuletinPemantauanKetahananPangan di Indonesia FokusUtama: Dampak El Niño. Vulume 2, Jan 2016. Accessed date : 2 February 2017. http://documents.wfp.org/stellent/groups/public/documents/ena/wfp281159.pdf

Monteith, J. L. (1965, July). Evaporation and environment. In Symp. Soc. Exp. Biol (Vol. 19, No. 205-23, p. 4).

Nasa (2015). NASA, NOAA Analyses Reveal Record-Shattering Global Warm Temperatures in 2015. Press Relase. Jan. 20, 2016. RELEASE 16-008. Accessed date 1 February 2017. https://www.nasa.gov/press-release/nasa-noaa-analyses-reveal-record-shattering-global-warm-temperatures-in-2015

Palmer, W. C., 1965: Meteorological drought. Office of Climatology Research Paper 45, Weather Bureau, Washington, D.C., 58 pp.

Pelton, W. L., King, K. M., & Tanner, C. B. (1960). An evaluation of the Thornthwaite and mean temperature methods for determining potential evapotranspiration. Agronomy Journal, 52(7), 387-395.

Piani, C., O. Haerter, and E. Corpola (2010), Statistical bias correction for daily precipitation in regional climate models over Europe, Theor. Appl. Climatol., 99, 187–192.

Schulzweida, U., Kornblueh, L., &Quast, R. (2006). CDO user's guide. Climate Data Operators, Version, 1(6).

Skamarock, W. C. Coauthors, 2008: A description of the advanced research WRF version 3. NCAR Tech. Note. NCAR/TN-475+ STR.

Syaukat, Y. (2011) The Impact of Climate Change On Food Production and Security and Its Adaptation Programs In Indonesia J. Issaas Vol. 17, No. 1:40-51.

Teutschbein, C., & Seibert, J. (2012). Bias correction of regional climate model simulations for hydrological climate-change impact studies: Review and evaluation of different methods. Journal of Hydrology, 456, 12-29.

Trenberth, K. E. (2011). Changes in precipitation with climate change. Climate Research, 47(1-2), 123-138.

Turco, M., von Hardenberg, J., Palazzi, E., Provenzale, A. (2015). REPORT:Regional climate projections and bias correction methods over the Greater Alpine Region, Accessed date 1 February 2017.http://www.nextdataproject.it/sites/default/files/docs/mos_ictp_prec_4.pdf

Van Den Besselaar, E.J.M., Van Der Schrier, G., Cornes, R., Aris Suwondo, I., & Klein Tank, A. M. G. (2016). SA-OBS: a daily gridded surface temperature and precipitation dataset for Southeast Asia. Royal Netherlands Meteorological Institute (KNMI), De Bilt, The Netherlands.

Van der Schrier, G., Jones, P. D., & Briffa, K. R. (2011). The sensitivity of the PDSI to the Thornthwaite and Penman-Monteith parameterizations for potential evapotranspiration. Journal of Geophysical Research: Atmospheres, 116(D3).

Van Der Schrier, G., Klein Tank, A. M., Van Den Besselaar, E. J., & Swarinoto, Y. S. (2016). Observed trends and variability in climate indices relevant for crop yields in Southeast Asia. Journal of Climate, 29(7), 2651-2669.

Van der Schrier, G., K. R. Briffa, P. D. Jones, and T. J. Osborn (2006), Summer moisture variability across Europe, J. Climate, 19, 2828–2834.

Van Vuuren, D. P., Edmonds, J., Kainuma, M., Riahi, K., Thomson, A., Hibbard, K., ... & Masui, T. (2011). The representative concentration pathways: an overview. *Climatic change*, *109*(1-2), 5.

Thornthwaite, C. W., 1948: An approach toward a rational classification of climate. Geogr. Rev.,38, 55–94.

Wells, Nathan, Steve Goddard, and Michael J. Hayes (2004). "A self-calibrating Palmer drought severity index." *Journal of Climate* 17.12 (2004): 2335-2351.

Wieder, W. R., Boehnert, J., Bonan, G. B., &Langseth, M. (2014). Regridded Harmonized World Soil Database v1. 2, Data set. Available on-line [http://daac. ornl. gov] from Oak Ridge National Laboratory Distributed Active Archive Center, Oak Ridge, Tennessee, USA.

Wilcke, R. A. I., Mendlik, T., &Gobiet, A. (2013). Multi-variable error correction of regional climate models. Climatic Change, 120(4), 871-887.

Wilks, D. (2011). Statistical Methods in the Atmospheric Sciences, 3rd Edition. Academic Press

Yang, H. (2015). Dynamic downscaling of climate change over the maritime continent. Accessed date 1 February 2017.http://adss.apcc21.org/DataSet/Cordex/CORDEX-SEA_25km.pdf
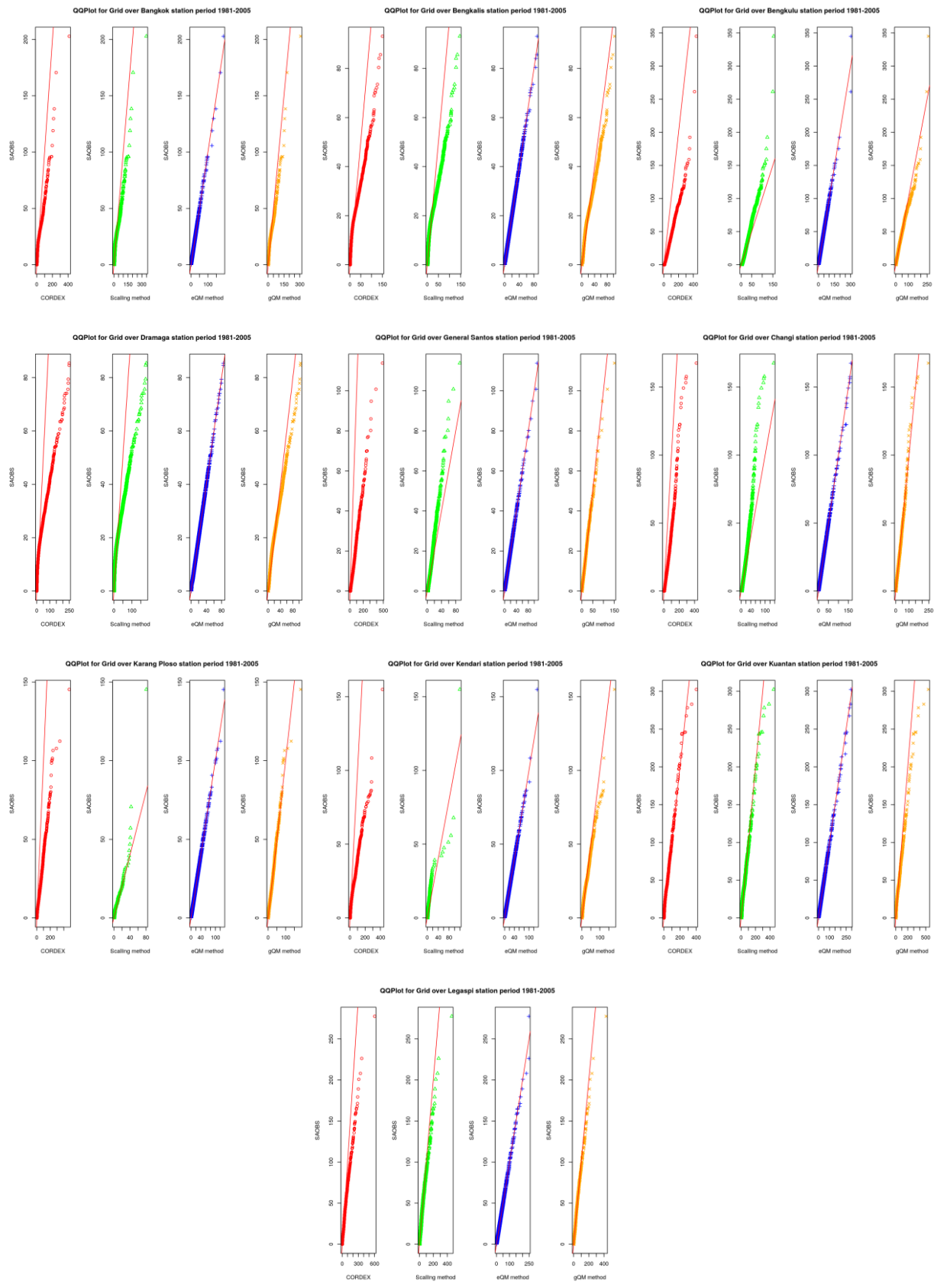
Appendix 1. QQplot bias corrected CORDEX-SEA by constructed daily CRU and by SA-OBS
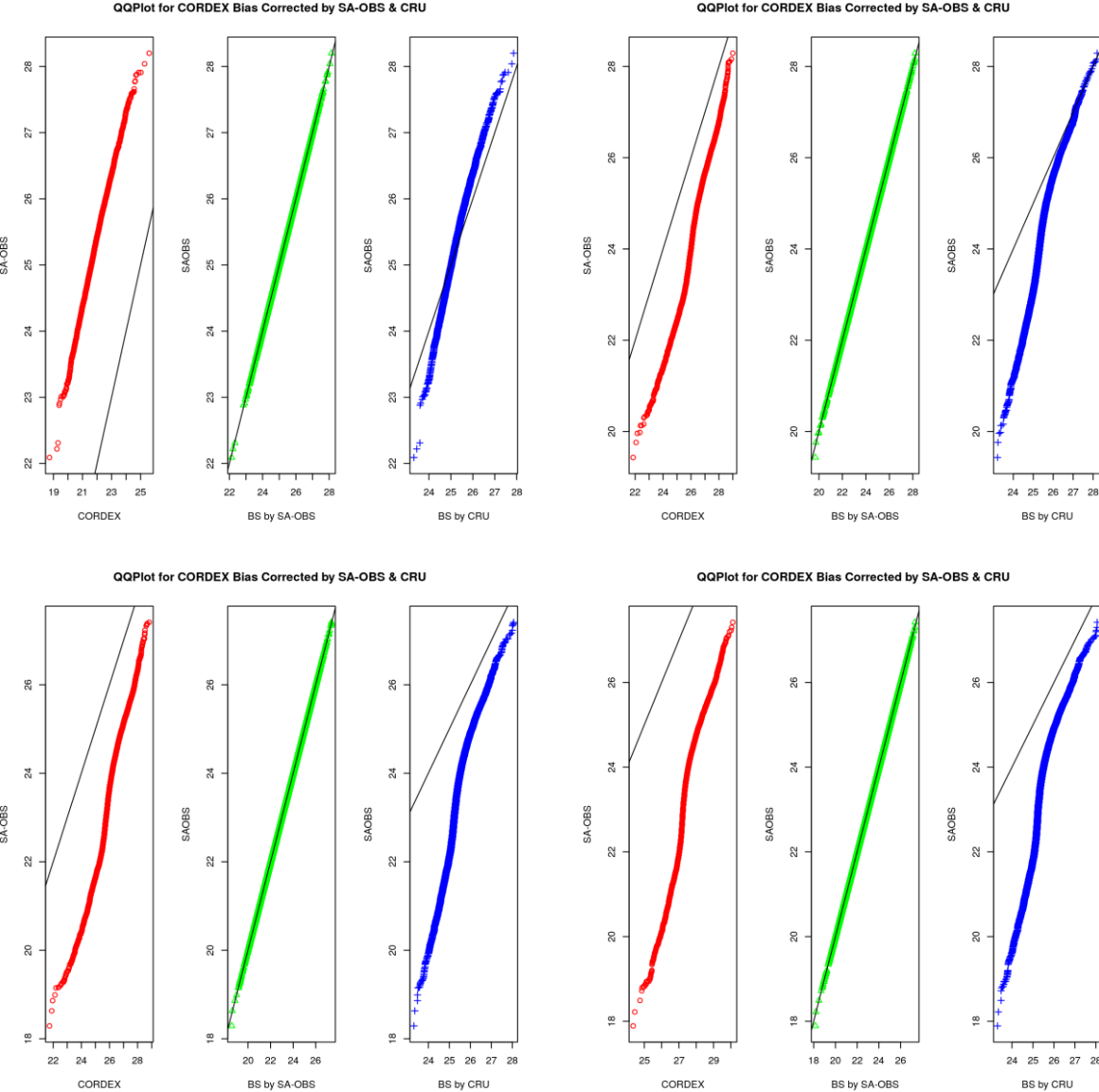
Appendix 2. ECDF bias corrected CORDEX-SEA by constructed daily CRU and by SA-OBS
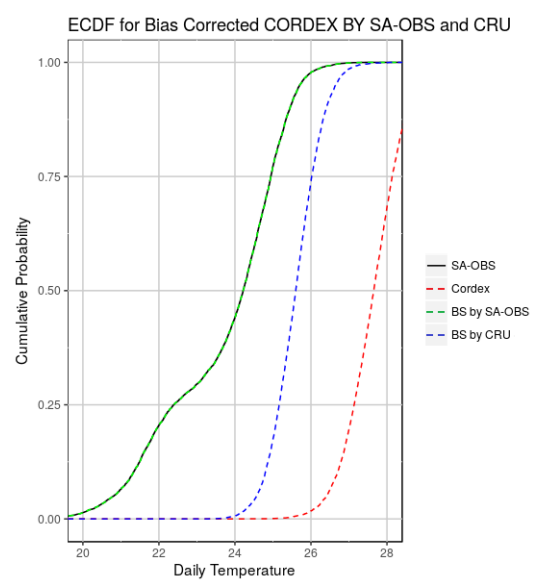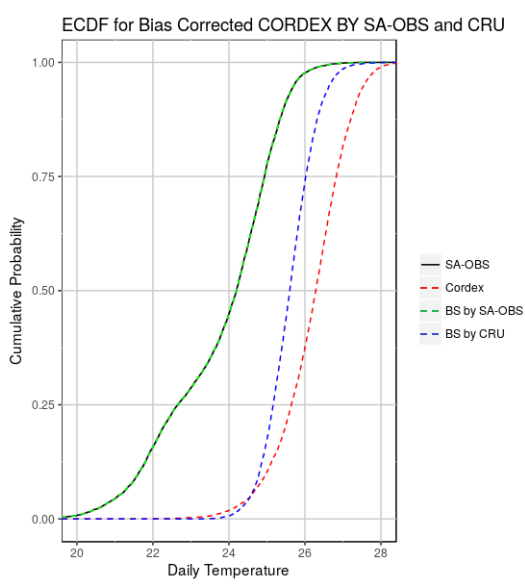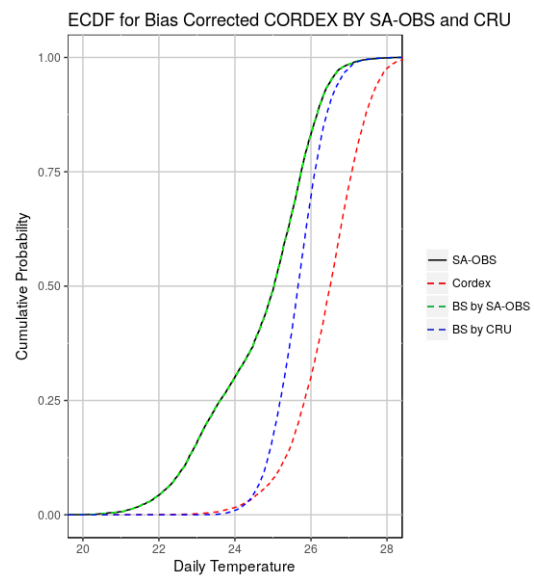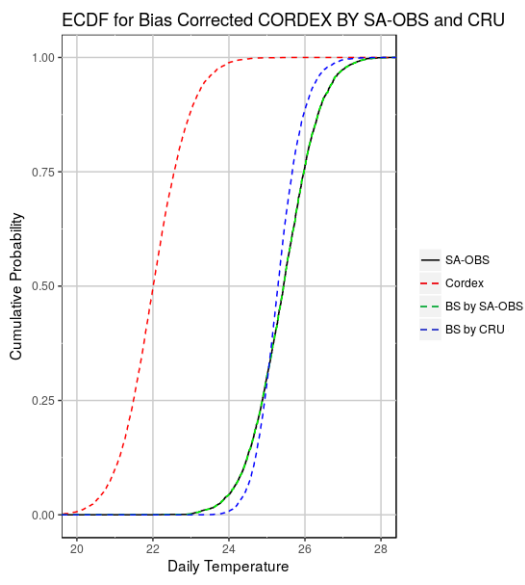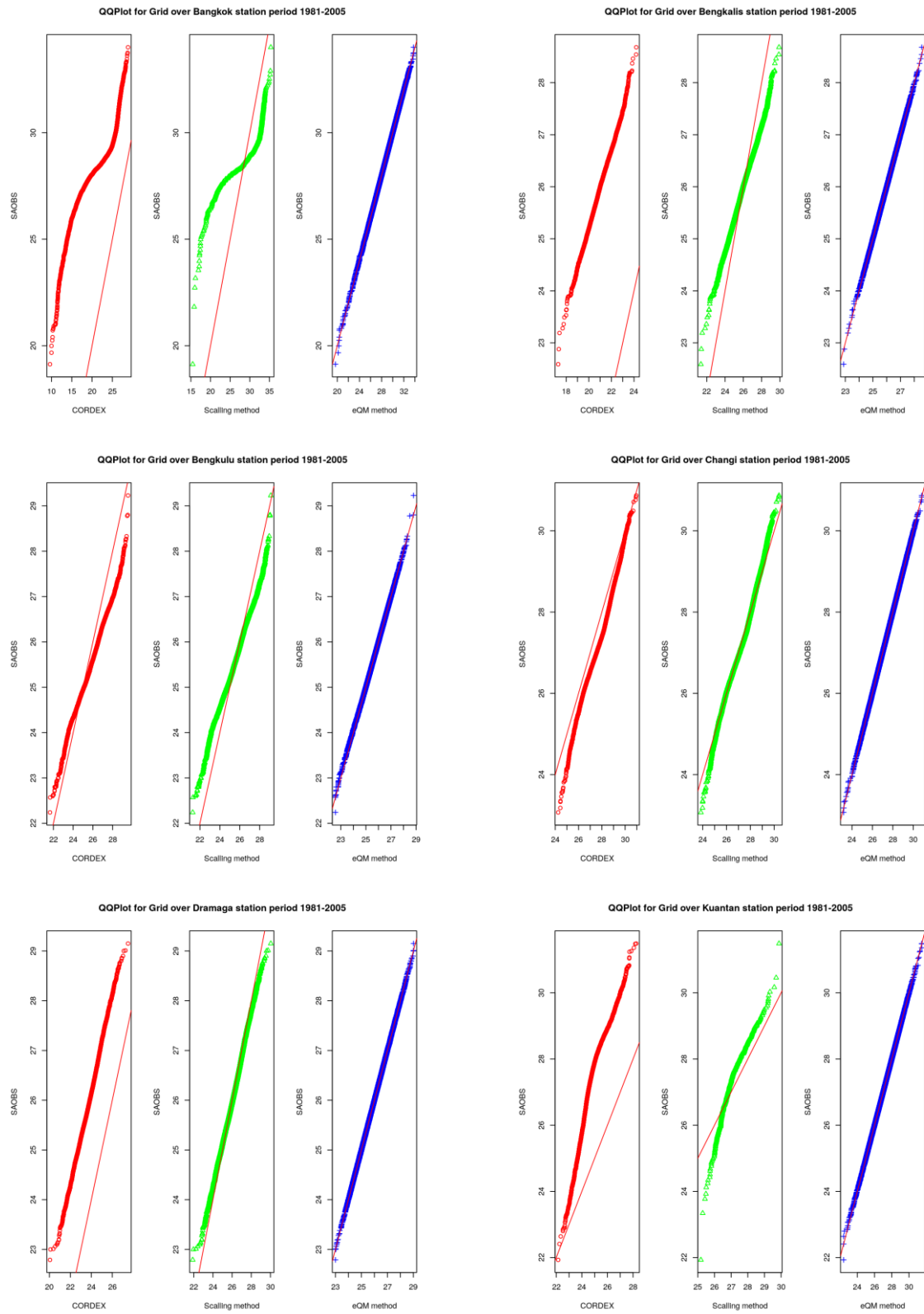
Appendix 3. QQplot of precipitation based on scaling (green), eQM (blue), and gQM (orange) bias correction methods for 10 stations in Southeast Asia for 1981-2005.

Appendix 4. ECDF of precipitation based on scaling (green), eQM (blue), and gQM (orange) bias correction methods for 10 stations in Southeast Asia for 1981-2005.
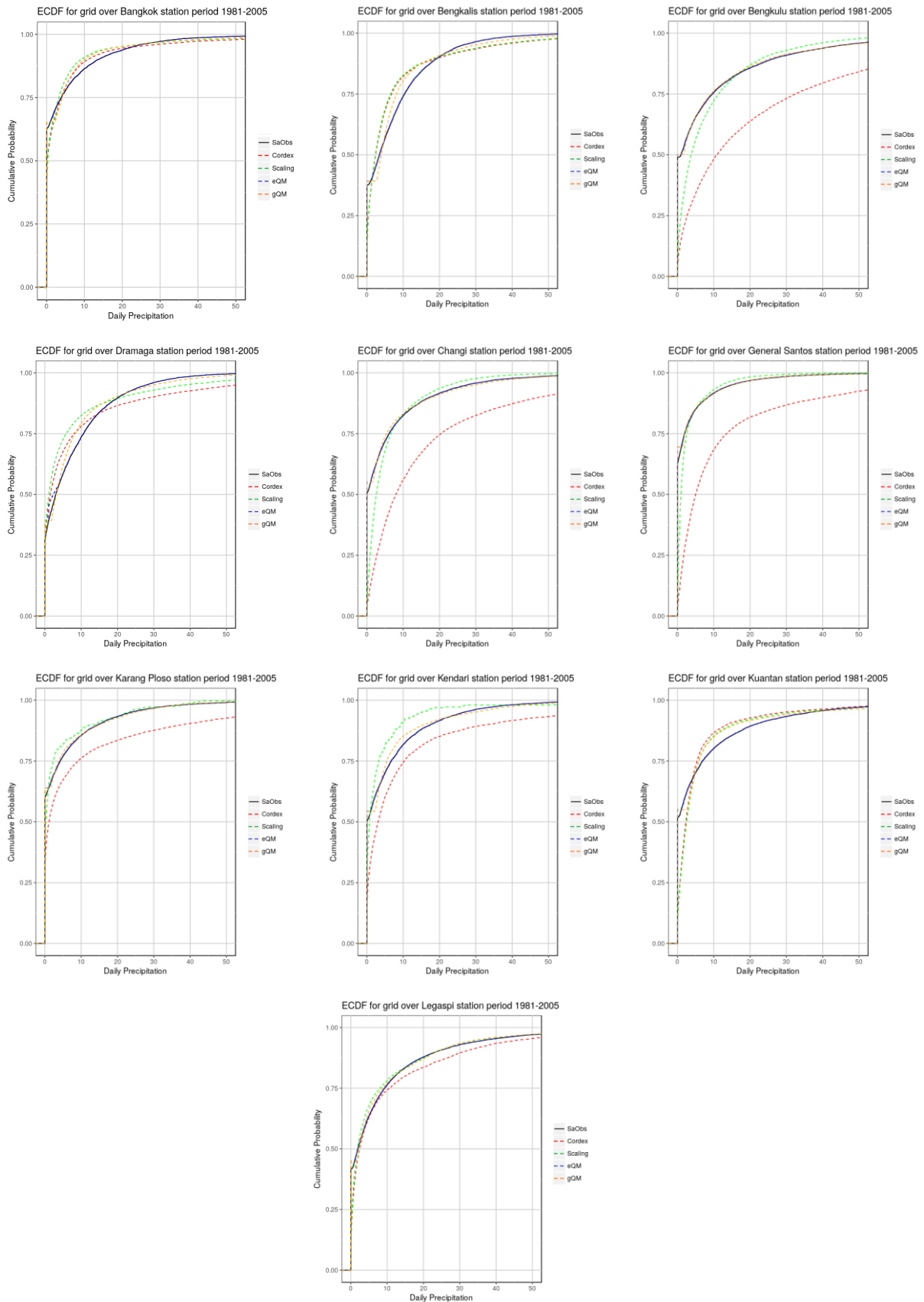
Appendix 5. QQplot of temperature based on scaling (green) and eQM (blue) bias correction methods for 6 stations in Southeast Asia for 1981-2005.

QQPlot for Grid over Bangkok station period 1981-2005

QQPlot for Grid over Bengkalis station period 1981-2005

QQPlot for Grid over Bengkulu station period 1981-2005

QQPlot for Grid over Changi station period 1981-2005

QQPlot for Grid over Dramaga station period 1981-2005

QQPlot for Grid over Kuantan station period 1981-2005

Appendix 6. ECDF of temperature based on scaling (green) and eQM (blue) bias correction methods for 6 stations in Southeast Asia for 1981-2005.
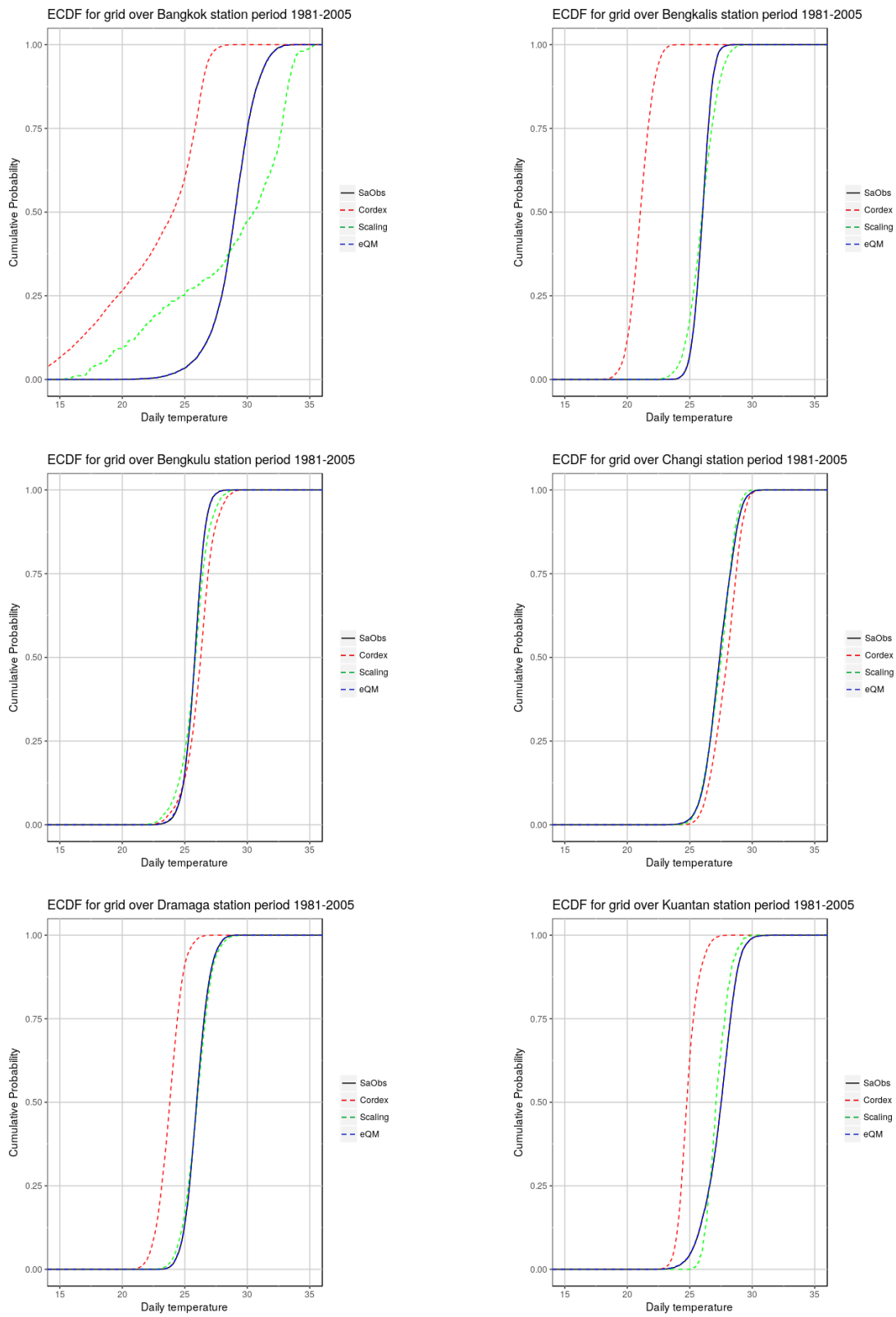
Appendix 7. Precipitation (SA-OBS) and temperature (CRU) anomaly during EN 1982, 1997 and 2015.

Precipitation anomaly

1982

1997

2015

Temperature Anomaly

1982

1997

2015
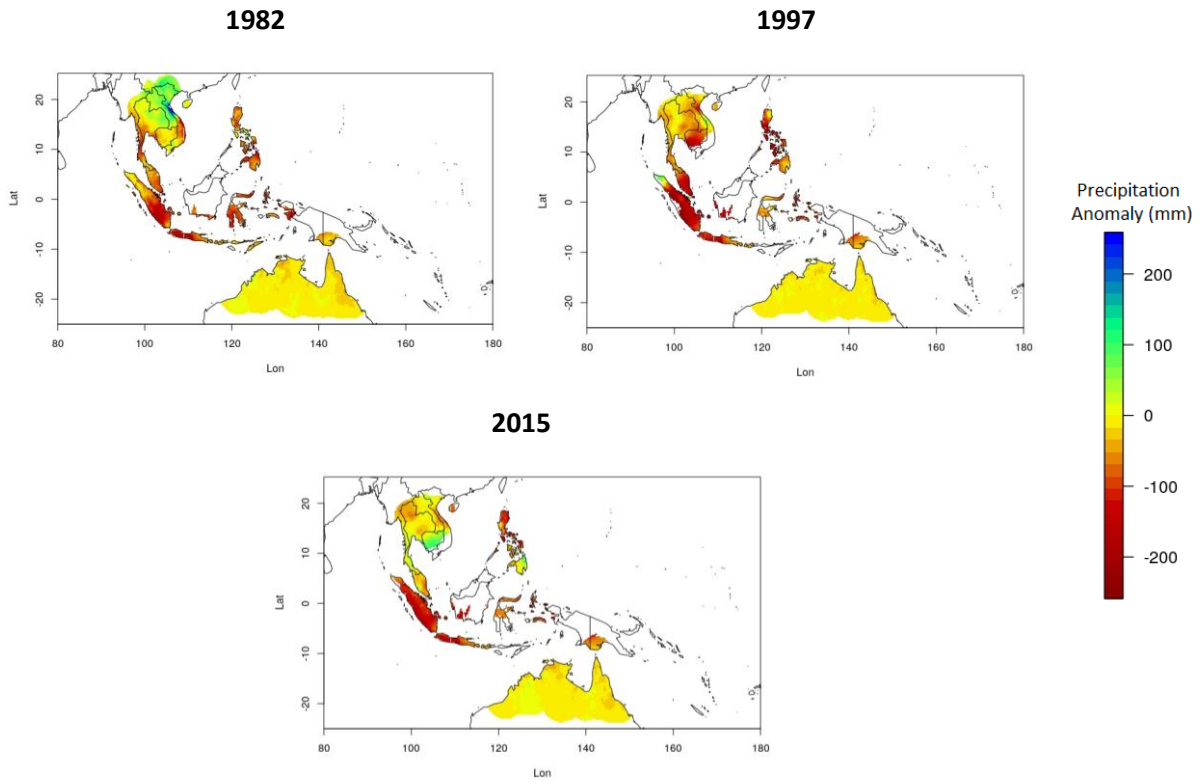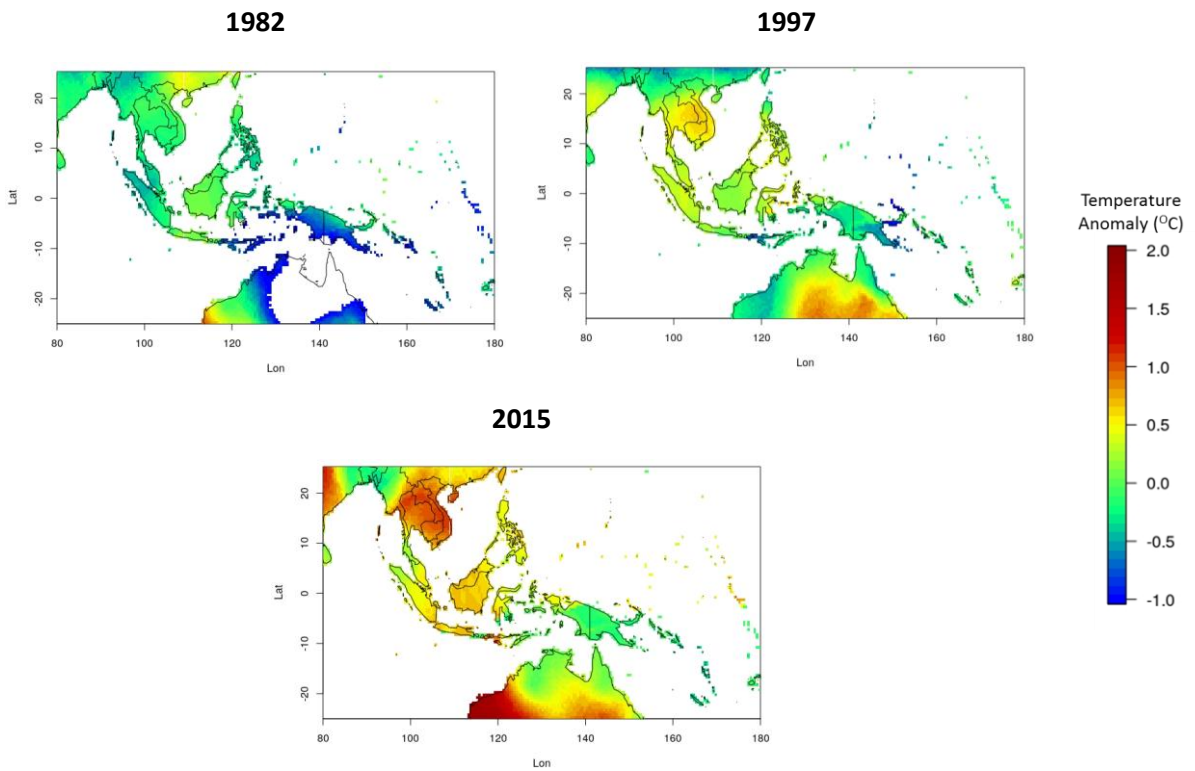
Appendix 8. Climatological condition of SON scPDSI for historical and future period. Historical period (a), Near future period under RCP4.5 (b) and RCP8.5 (c). Far future period under RCP4.5 (d) and RCP8.5 (e)

a.
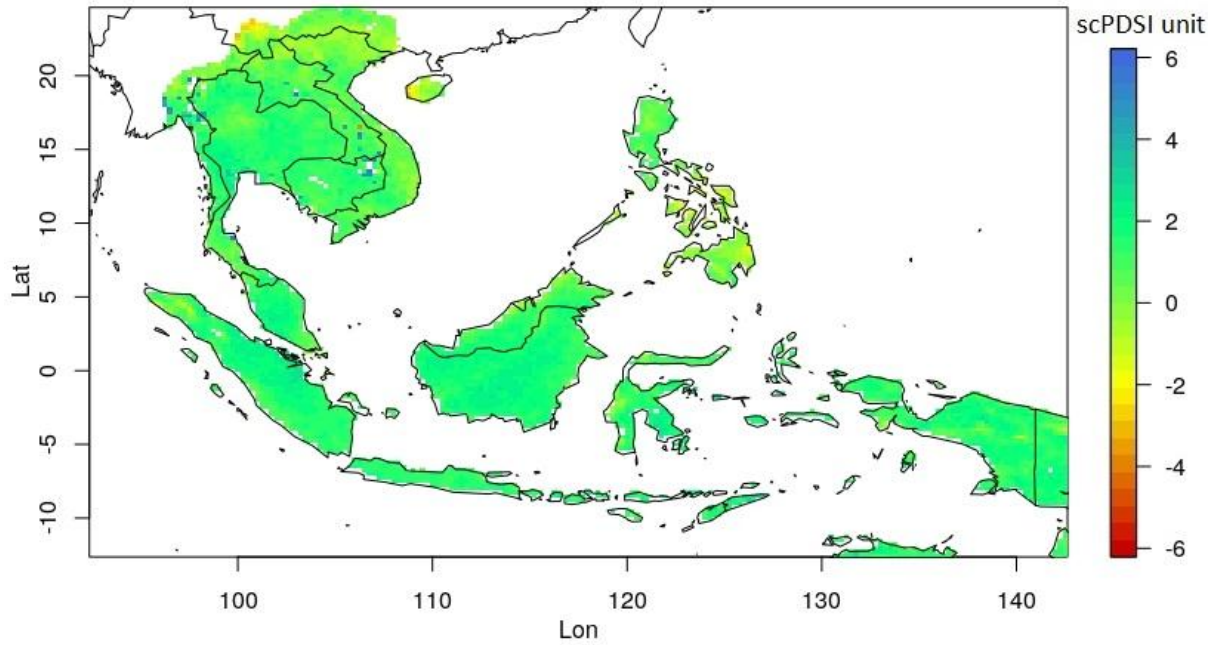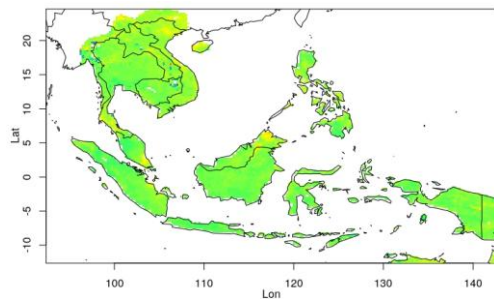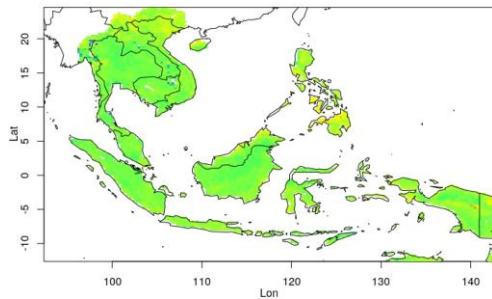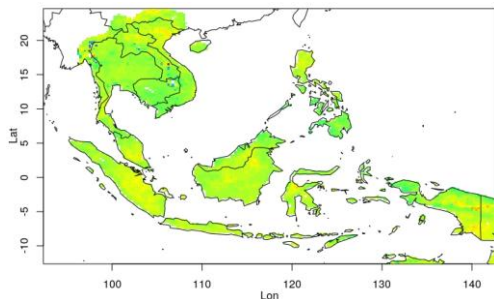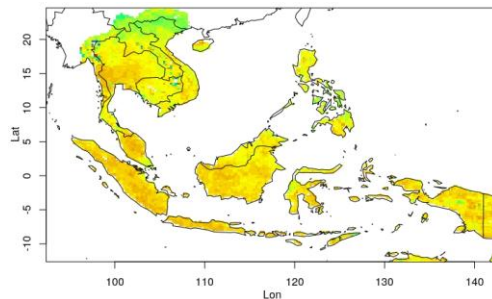
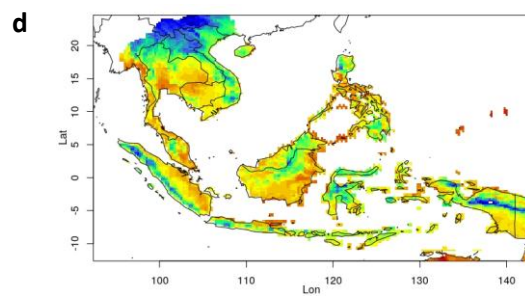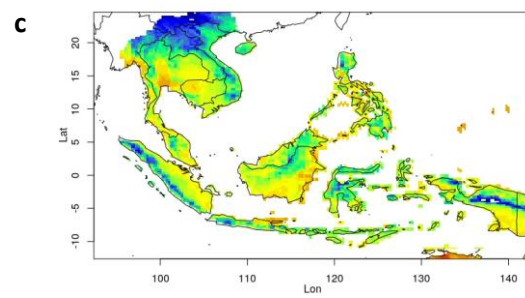**Appendix 9**. Climatological condition of SON precipitation. Historical period (a), NF-4.5 (b), NF-8.5 (c), FF-4.5 (d) and FF-8.5 (e).
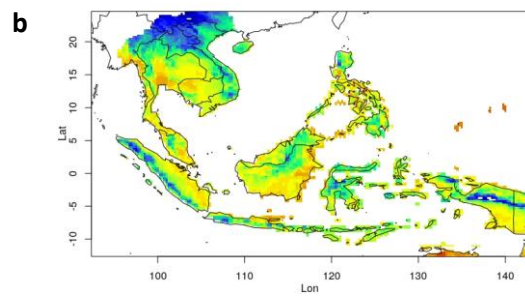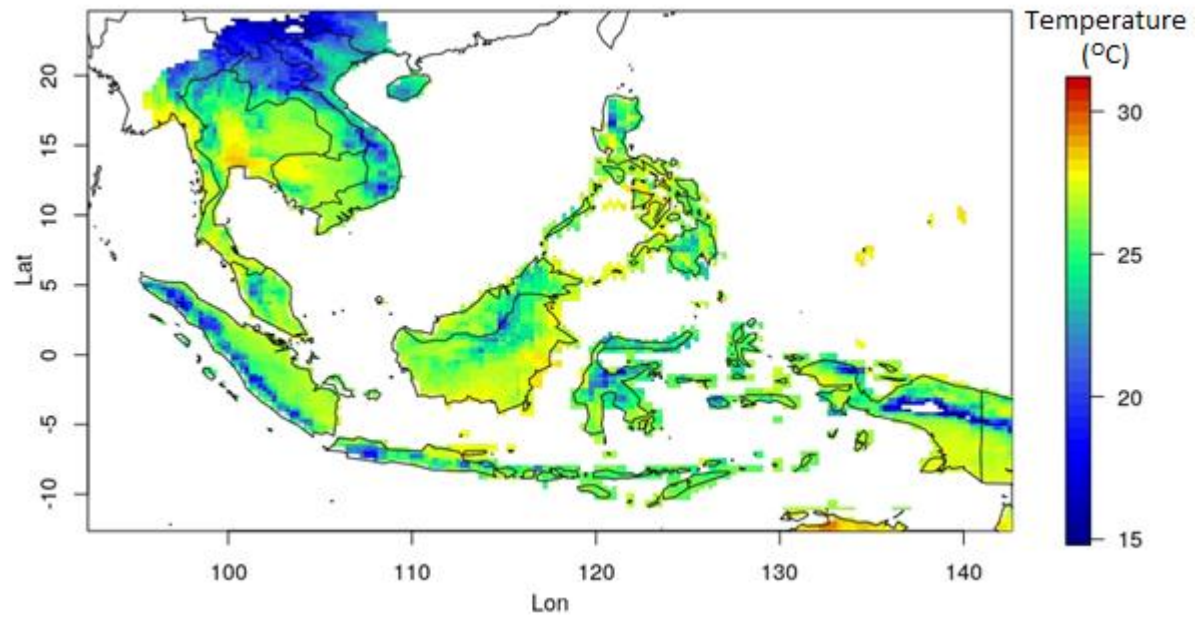
a.
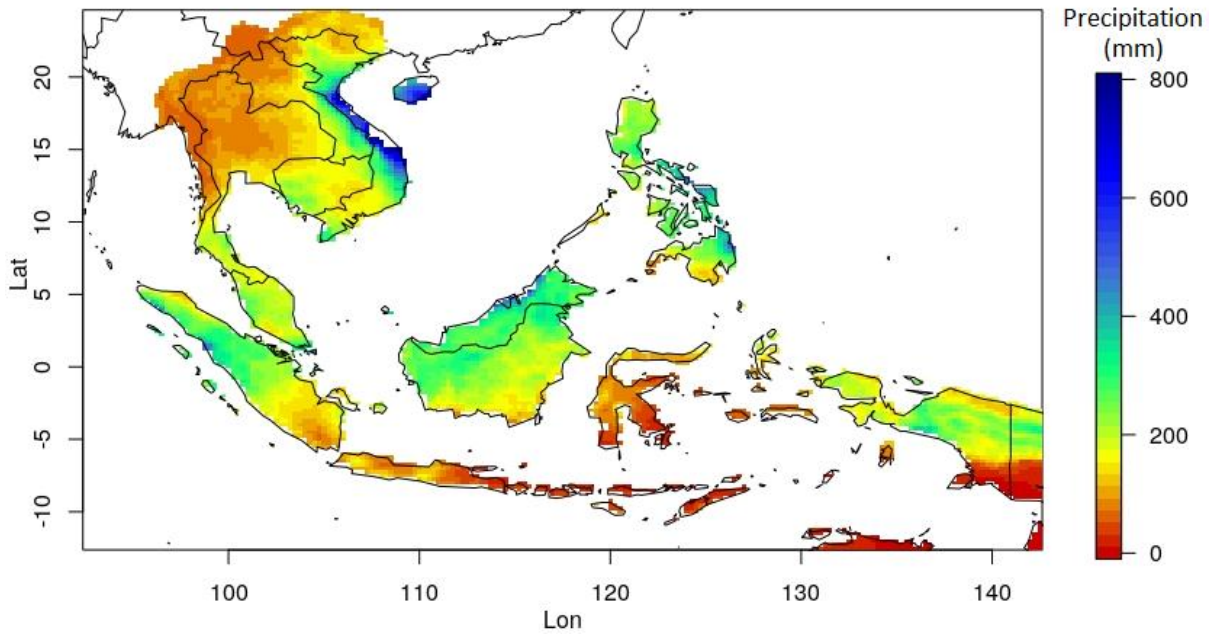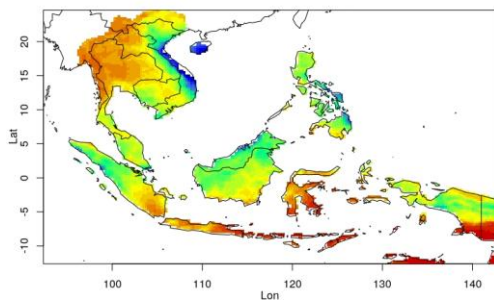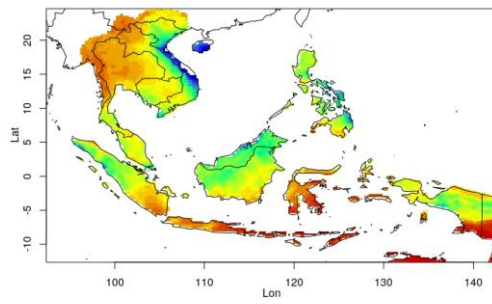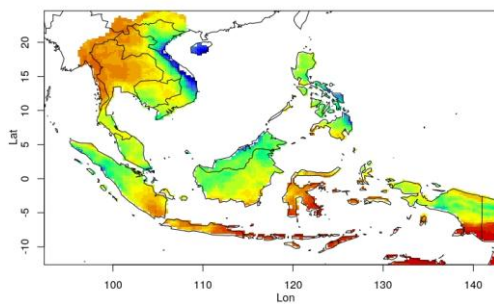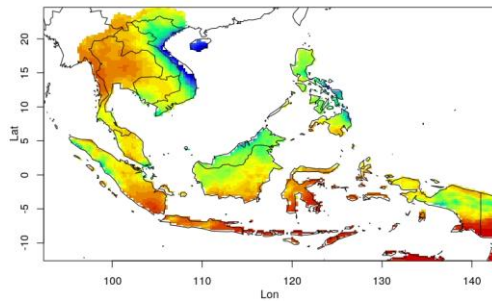
Appendix 10. Climatological condition of SON temperature. Historical period (a), NF-4.5 (b), NF-8.5 (c), FF-4.5 (d) and FF-8.5 (e).

a.
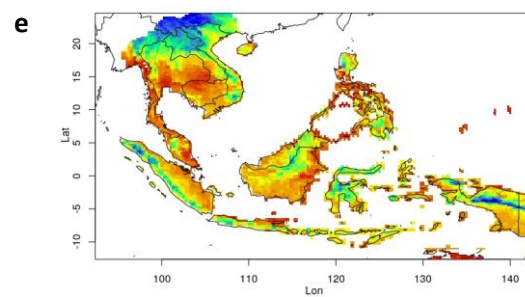
Appendix 11. Temperature anomaly for SON in future period under RCP4.5 and RCP8.5. Near future period under RCP4.5 (a) ans RCP8.5 (b). Far future period under RCP4.5 (c) ans RCP8.5 (d)